Accepted Manuscript

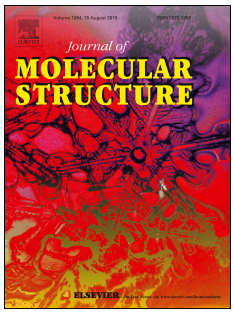

Pharmacophore modeling and conformational analysis in the gas phase and in aqueous solution of regioisomeric melatonin analogs. A theoretical and experimental study

Humberto Mendoza-Figueroa, Gelacio Martínez-Gudiño, Jorge E. Villanueva-Luna, Joel J. Trujillo-Serrato, Martha S. Morales-Ríos

PII: S0022-2860(16)31353-9

DOI: 10.1016/j.molstruc.2016.12.040

Reference: MOLSTR 23238

To appear in: *Journal of Molecular Structure*

Received Date: 12 August 2016

Revised Date: 8 December 2016

Accepted Date: 14 December 2016

Please cite this article as: H. Mendoza-Figueroa, G. Martínez-Gudiño, J.E. Villanueva-Luna, J.J. Trujillo-Serrato, M.S. Morales-Ríos, Pharmacophore modeling and conformational analysis in the gas phase and in aqueous solution of regioisomeric melatonin analogs. A theoretical and experimental study, *Journal of Molecular Structure* (2017), doi: 10.1016/j.molstruc.2016.12.040.

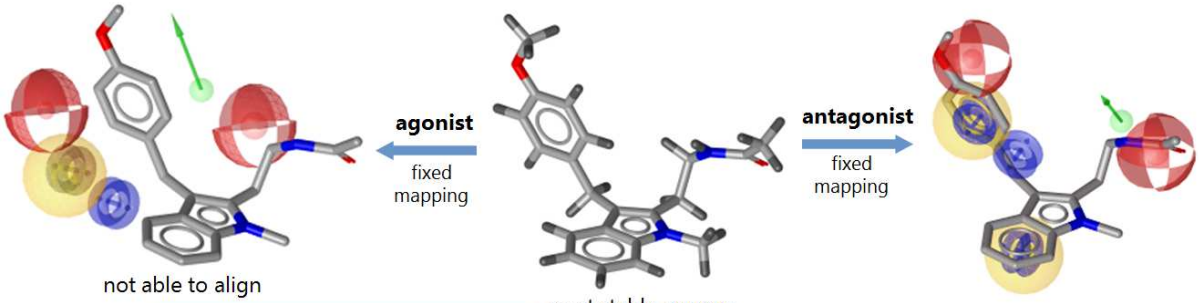

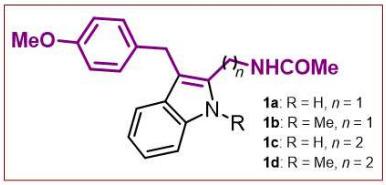

Pharmacophore modeling and conformational analysis in the gas phase and in aqueous solution of regioisomeric melatonin analogs. A theoretical and experimental study

Humberto Mendoza-Figueroa[a], Gelacio Martínez-Gudiño[a], Jorge E. Villanueva-Luna[a], Joel J. Trujillo-Serrato[b], Martha S. Morales-Ríos[a,*]

[a] Departamento de Química and [b] Programa de Posgrado en Farmacología, Centro de Investigación y de Estudios Avanzados del Instituto Politécnico Nacional, Apartado 14-740, Mexico City, 07000 Mexico.

Abstract

In this work, 2-(*N*-acylaminoalkyl)indoles **1a**-**1d**, that incorporate a *p*MeOBn group at the 3-position of the indole ring were virtual screened as potential melatoninergic ligands by analog-based design study using pharmacophore modeling. Pharmacophore models for melatoninergic agonist and antagonist activity were developed in order to identify the molecular constraints that define the geometric relationship among chemical features in each model. The best hypothesis consisted of six features for agonists and eight features for antagonists. The models suggest that the agonists and antagonists can share the same 3D arrangement for the six common pharmacophoric elements identified: two hydrogen bond acceptors (HBA), one hydrogen bond donor (HBD), one hydrophobic area (H), and two aromatic rings (AR). The extra hydrofobic interaction might be used as criterion for identified the pharmacological antagonist profile. Based on the pharmacophore fit, it was found that structures **1c** and **1d** show a good structural overlay that meets the requirements for the antagonistic pharmacophore hypothesis. Molecular modeling studies using the PCM solvation model predicted that the most stable conformers of **1a**-**1d** match the antagonist pharmacophore hypothesis in contrast to those in the gas phase. Structures **1a**-**1c** were synthesized only but the activities were not tested.

Keywords: 2-(*N*-acylaminoalkyl)indoles, synthesis, virtual screening, pharmacophore modeling, gas-phase, continuum solvent

*Corresponding author. *E-mail address*: smorales@cinvestav.mx (M. S. Morales-Ríos)

1. Introduction

Melatonin (5-methoxy-*N*-acetyltryptamine), hormone primarily secreted by the pineal gland, has wide functions in vertebrate organisms, with effects almost on all tissues and organs [1-3]. Melatonin production and secretion are regulated by sunlight sensed by the eyes and control circadian rhythms. This hormone has a complex mechanism of action. It can cross the cell plasma membrane and exert its actions in all cells of the body. Most of the regulatory functions exerted by this hormone are mediated by two high-affinity G-protein-coupled receptors, named MT1 and MT2 [4], which have been recognized as promising targets in the treatment of a number of human diseases and disorders. Melatonin modulates neurogenesis, synaptic functions, neuronal cytoskeleton and gene expression [5]. Additionally, melatonin is a powerful endogenous antioxidant involved in the prevention of the oxidative stress both through its direct free radical scavenging effect and by increasing antioxidant activity [6-10]. Therefore, a lot of experimental and theoretical work has been devoted to understanding the molecular mechanisms underlying such unique properties of melatonin and of alternate molecules capable of mimicking its effects [11].

Previous studies on a great number of structurally different MLT receptor ligands, which range from simple indole derivatives and their bioisosteres to phenylalkyl amides and constrained melatoninergic agents [12], have demonstrated that suitably spaced alkoxyaryl core and the amido side chain seem to be critical in determining the binding affinity and biological activity of these melatoninergic ligands [13-17]. In this line, structure activity relationship studies of regioisomeric melatonin-based analogues in which the MLT side chain was shifted from the C-3 to the either the N-1 or to the C-2 indole position, allowed to the development of indole MLT agonist and antagonist compounds, provided they keep an appropriate spatial relationship of its pharmacophoric groups (*i.e*. the aromatic moiety, the methoxy substituent and the amido group) [18].

We now report a virtual screened of a series of 2-(*N*-acylaminoalkyl)indole derivatives **1a-1d** bearing a methoxyaryl group separated by an indole ring spacer from the secondary amide, as potential melatoninergic ligands. Their structure design was based on pharmacophore mapping study using available agonists and antagonists for melatonin receptors. Because compounds **1a-1d** have hydrogen bond donor and acceptor sites, their conformational stability in the gas phase and in continuum solvent was also analyzed. The most stable conformers in continuum solvent were spatial superposed with the pharmacophore models and served to validate the obtained results. The synthesis of compounds **1a-1c** has been performed. The structure, atom numbering scheme, and dihedral angle definitions of studied compounds **1a-1d** are displayed in Fig. 1.

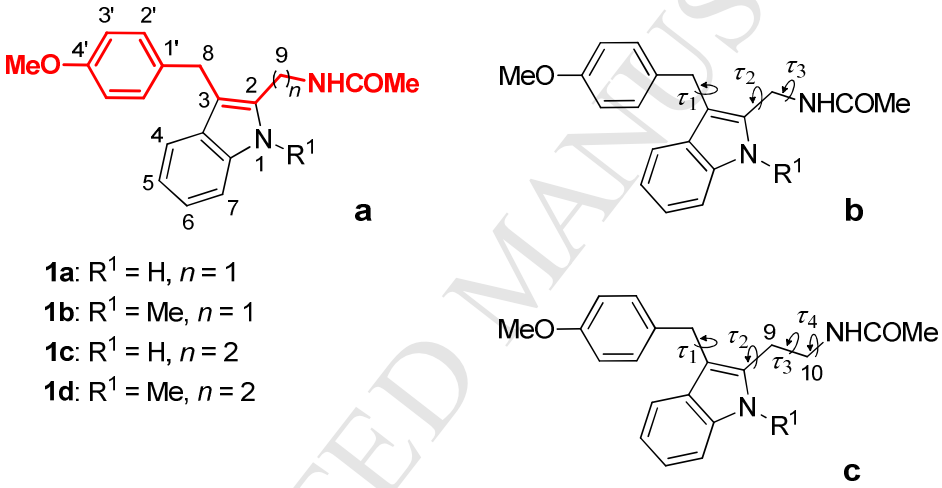

Fig. 1. (a) Structures of compounds **1a-1d** and numbering. The indole nitrogen atom is designated as N_1 and the amide nitrogen as N_2. Minimal structural requirements for the biological activity of melatoninergic ligands are shown in bold. (b) Dihedral angle definitions for **1a** and **1b**: $\tau_1 = \angle(C_2C_3C_8C_{1'})$; $\tau_2 = \angle(C_3C_2C_9N_2)$; $\tau_3 = \angle(C_2C_9N_2C_{=O})$. (c) Dihedral angle definitions for **1c** and **1d**: $\tau_1 = \angle(C_2C_3C_8C_{1'})$; $\tau_2 = \angle(C_3C_2C_9C_{10})$; $\tau_3 = \angle(C_2C_9C_{10}N_2)$; $\tau_4 = \angle(C_9C_{10}N_2C_{=O})$.

2. Results and discussion

2.1. Pharmacophore modeling

Pharmacophore mapping methodology based on 3D alignments of the pharmacophore features of already known active molecules acting as agonists and antagonists for melatonin receptors was explored in order to predict whether indolylbenzylamides **1a**-**1d** meet the requirements of the pharmacophore hypotheses and therefore could function as potential melatoninergic ligands. In addition, the goal was to estimate to what extent the pharmacophore maps could be valuable in dissecting important features for the modeling of new melatoninergic ligands with agonist or antagonist profiles. Pharmacophore features were identified based on representative training sets of 8 agonists and 8 antagonists. The selection of these molecules was supported on their structural diversity, affinity and potency (Supporting Information). Screens were carried out using the LigandScout 3.12 [19] program for automatic generation of the hypotheses, which were scored by setting root mean square deviation (RMSD) below 1.0, and using default parameters.

The generated agonist and antagonist models were analyzed using several criteria: (i) the number of pharmacophoric elements, (ii) the RMSD fit of corresponding pharmacophoric elements, (iii) the degree of overlap of molecular volumes, and (iv) the distances between pharmacophore features. The agonist top hypothesis was composed of six essential features for activity: two hydrogen bond acceptors (HBA); one hydrogen bond donor (HBD); one hydrophobic area (H); and two aromatic ring features (AR). In Fig. 2, the pharmacophoric elements allow a certain spherical tolerance surrounding the ideal position of a particular feature in 3D space. The results were consistent with a previously developed melatonin receptor ligands model [20-24].

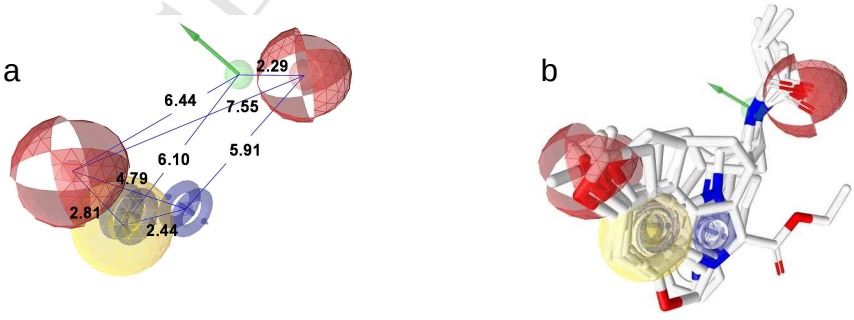

Fig. 2. (a) 6-Points pharmacophore model, key features include HBA (red), HBD (green), H (yellow), and AR (blue), distance relation in Å. (b) Superposition of the 8 representative agonist melatoninergic compounds on the 6-points pharmacophore model.

The antagonist pharmacophore hypothesis is shown in Fig. 3. In this case, the best quality option was composed of eight key features, six of which are in common with the agonist model above described. The extra hydrophobic interaction identified as a ring aromatic feature, might contribute to conferring antagonist activity. These results suggest that agonists and antagonists can share the same arrangement for their mutual pharmacophoric features in agreement with previously prediction [25].

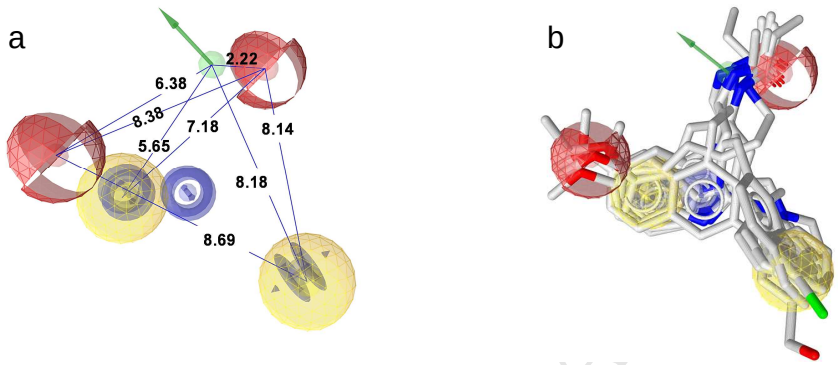

Fig. 3. (a) 8-Points pharmacophore model, key features include HBA (red), HBD (green), H (yellow), and AR (blue), distance relation in Å. (b) Superposition of the 8 representative antagonist melatoninergic compounds on the 8-points pharmacophore model.

The 3D-pharmacophore models for melatoninergic agonist and antagonist activity were then used for the prediction of melatoninergic activity of indolylbenzylamides **1a-1d**. The test set molecules were flexibly aligned with the chemical features of the models and the inspection of the resulting structural superpositions showed the best-fit with the antagonist pharmacophore hypothesis, (Supporting Information) largely because the hydrophobic benzyl center has no comparable constituent in the agonist model. As shown in Fig. 4, the antagonist model identified the following six mutual pharmacophoric elements in **1a-1d**: one HBA (the amide oxygen); one HBD (the amide hydrogen); two H (the hydrophobic part of the indole ring and the benzyl group); and two AR (the benzene part of the indole ring and the benzyl group). The results suggest that the hydrophobic benzyl center led to compounds with antagonistic properties. This hypothesis obviously needs to be supported by further experimental data. In addition, compounds **1c** and **1d** showed superior structural overlay with the antagonist model compared to **1a** and **1b** in the

series. Shortening the acetyl side chain by a methylene could prevent the proper alignment of **1a** and **1b**.

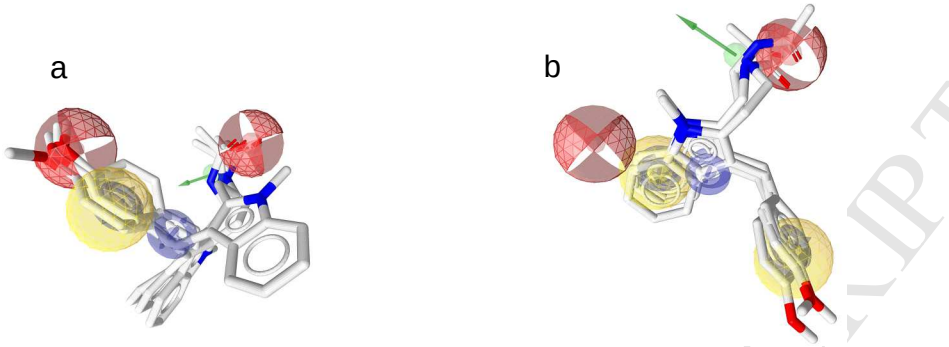

Fig. 4. Alignment of indolylbenzylamides **1a-1d** with the chemical features of (a) agonist model (b) antagonist model.

2.2. Conformational Analysis

Analysis of the conformational stability of **1a-1d** structures is important especially when these molecules can be involved in attractive intramolecular N–H···O or NC–H···O H-bond interactions. One of the main questions has always been whether intramolecular H-bonds, which are supposed to exist in some gas-phase conformations, are maintained after aqueous solvation. Therefore, taking into account that the aqueous phase results better simulate the biological environment, the structural parameters of the lower energy 3D structures of **1a-1d** in the gas phase and aqueous solution were comparatively studied. All computational optimizations were carried out by using the Gaussian 03 or 09 program package [26,27]. The characterization of the minimum energy conformers in gas phase (C_g) or aqueous solution (C_s) of **1a-1d** (Gibbs energies among conformers, expressed in relative terms, the respective mole fractions given by the Boltzmann populations, and relevant dihedral angles) are presented in Table 1. The absolute values for the lowest Gibbs energy conformer of every compound are given in Table 2, while the corresponding distances (*d*, *D*) and angular parameters (θ, φ) used in the description of H-bonds are given in Table 3. The schematic drawing of the most stable conformers of **1a-1d** in the gas phase are given in Fig. 5, while those in the presence of the implicit water solvent are given in Fig. 6.

2.2.1. Gas Phase

Analysis of the distances (*d*, *D*) and angular parameters (θ, φ) (Table 3) suggests that the conformational stability of **1a**-**1d** in the gas phase is affected by attractive intramolecular N–H···O or NC–H···O H-bond interactions. In the most stable two pair of specular C_ga1/C_ga1′ and C_ga2/C_ga2′ conformations of **1a**, carrying 91% of the total population, the arrangements make possible the formation of an intramolecular N–H···O hydrogen bond between the indole sp^2-NH proton and the O atom of the carbonyl amide group, closing a seven-membered ring, as assigned for the relatively short N–H···O < 2.2 Å distances (Table 3). As a result, the amidomethyl side chain is fairly rigid. Therefore, the main conformational freedom involves the rotation of the aromatic methoxy group which was close to 0° or 180° owing to the resonance with the benzyl group (Fig. 5). While for the homologue **1c**, six most stable conformers were identified. The C_gc1 conformation and the pair of specular C_gc2/C_gc2′ conformations, contributing over 90% of the total population, are stabilized by an eight-membered intramolecular H-bond, as assigned for the relatively short N–H···O < 2.1 Å distances (Table 3). The aforementioned hypothesized cyclic H-bond formation delivers significant stability to the particular structure in the gas phase. Concerning the minimum energy conformers found for the *N*-methyl derivatives **1b** (C_gb1 and C_gb2) and **1d** (C_gd1/C_gd1′ specular pair) with highest abundance (a Boltzman population density greater than 85%), show that they exhibited typical directional features between the *N*-methyl group and the oxygen atom of the carbonyl amide group in concordance with the formation of a carbon-oxygen N–CH···O hydrogen bonding. H-bond (*d*) and carbon-oxygen distances (*D*) in the minimum energy conformations of **1b** and **1d** are within the typical van der Waals distances: $d_{C–H\cdots O}$ = 2.7 Å; *D* = 3.7 Å, frequently used as cutoffs for C–H···O hydrogen bond identification[28-31] (Table 3).

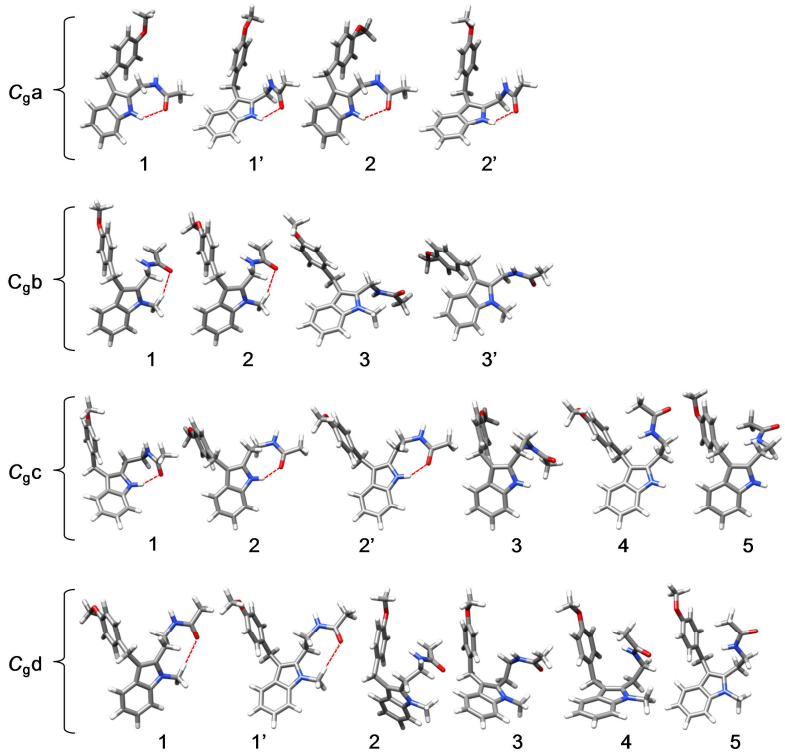

Fig. 5. Geometries for the minimum energy conformers in the gas phase found for **1a** (C_ga), **1b** (C_gb), **1c**, (C_gc) and **1d** (C_gd). The stability increases from right to left in each row. Specular conformations, with the same absolute values of dihedral angles (τ) but opposite signs, were found for the minimum energy conformers of **1a** (C_ga1/C_ga1′; C_ga2/C_ga2′), **1b** (C_gb3/C_gb3′), **1c** (C_gc2/C_gc2′), and **1d** (C_gd1/C_gd1′). Intramolecular H-bonding is indicated as a red dashed line.

2.2.2. Aqueous Solution

Analysis of the dihedral angles (Table 1) as well as the corresponding lengths (*d*, *D*), and angular preferences (θ, φ) of H-bond interactions (Table 3) provides evidence that the structural parameters of the conformers of **1a** in vacuo, namely C_ga1/C_ga1′and C_ga2/C_ga2′, (Fig. 5) or in solution C_sa1 and C_sa2 (Fig. 6) are not much different. The exception are the dihedral angles characterizing the orientation of the benzyl group. The relatively short N–H···O < 2.3 Å distance (Table 3)in conformers C_sa1 and C_sa2, carrying 100% of the total population, suggested the presence of intramolecular H-bond. Therefore, the intramolecular N–H···O H-bond supposed to existin gas-phase remains after aqueous solvation. In contrast, as can be seen in Tables 1 and 3, the solvent environment modify

severely the geometries of the conformers of **1b**-**1d** altering the dihedral angles involved in the intramolecular H-bond interaction predicted in the corresponding gas phase structures. As a result of these geometric changes, the stabilizing intramolecular H-bond force important in the gas-phase is breaking in water to enable the formation of intermolecular H-bonds with solvent molecules. It is of further interest to observe that in the ^{1}H NMR spectra, recorded in $CDCl_3$, δN_1H for **1a** at 8.90 occurs 0.38 ppm high frequency from δN_1H of **1c** at 8.52 (Table 4), consistent with the assumption that an amount of intramolecular H-bonding is present in **1a** [32]. The change of solvent from $CDCl_3$ to DMSO-d_6 moves the N_1H indole and N_2H amide resonance proton signals at higher-frequency (Table 4), indicating the formation of intermolecular H-bonding between the NH groups and solvent DMSO.

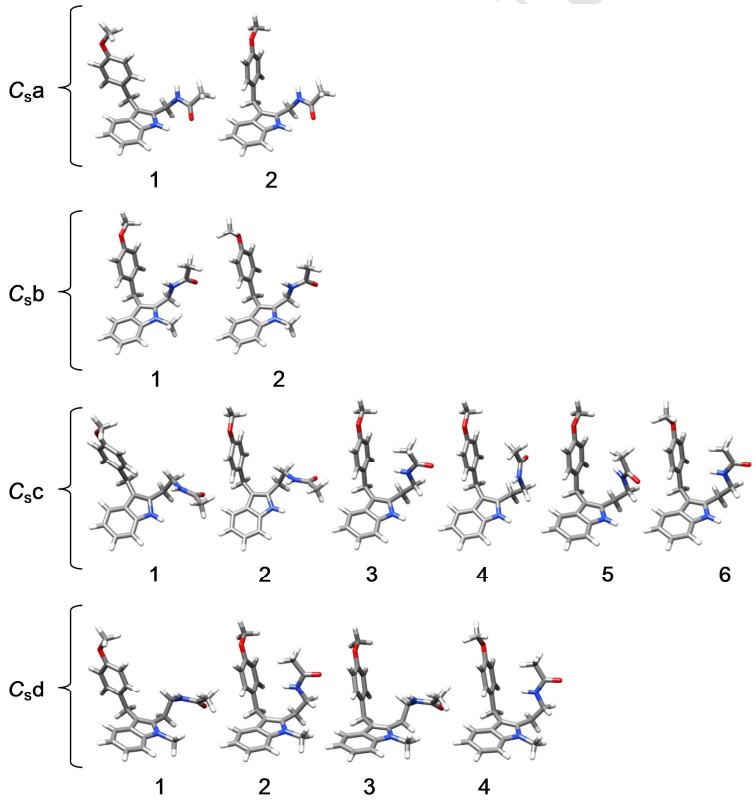

Fig. 6. Geometries for the minimum energy conformers in the aqueous solution found for **1a** (C_sa), **1b** (C_sb), **1c**, (C_sc) and **1d** (C_sd). The stability increases from right to left in each row.

Table 1

Relative Gibbs energies in the gas phase ($G_{gas,rel}$) and in aqueous solution ($G_{soln,rel}$), molar fractions (χ, %), and selected dihedral angles (τ, °) for the minimum energy conformers of **1a**-**1d**.[a]

	gas phase							aqueous solution						
	$G_{gas,rel}$[b]	χ_{gas}[c]	τ_1[d]	τ_2[d]	τ_3[d]	τ_4[d]		$G_{soln,rel}$[b]	χ_{soln}[c]	τ_1[d]	τ_2[d]	τ_3[d]	τ_4[d]
1a							**1a**						
C_ga1	0.00	28.36	55.2	-108.5	-77.2	-	C_sa1	0.00	74.57	-111.2	115.4	79.6	-
C_ga1′	0.00	28.36	-55.3	108.5	77.2	-	C_sa2	0.64	25.43	-82.3	112.7	78.8	-
C_ga2	0.16	21.64	68.5	-108.4	-77.0	-	-	-	-	-	-	-	-
C_ga2′	0.16	21.64	-68.6	108.4	77.0	-	-	-	-	-	-	-	-
1b							**1b**						
C_gb1	0.00	46.68	68.5	-92.0	-110.4	-	C_sb1	0.00	58.35	-78.7	105.1	164.4	-
C_gb2	0.08	40.59	73.3	-90.9	-109.1	-	C_sb2	0.20	41.65	-81.2	105.6	159.4	-
C_gb3	1.18	6.36	-110.3	-104.8	-120.6	-	-	-	-	-	-	-	-
C_gb3′	1.18	6.36	110.3	104.8	120.6	-	-	-	-	-	-	-	-
1c							**1c**						
C_gc1	0.00	42.59	-75.6	158.7	-60.1	107.1	C_sc1	0.00	42.17	112.3	92.1	61.8	88.9
C_gc2	0.35	23.47	80.9	-119.2	-124.2	74.8	C_sc2	0.32	18.68	-82.8	95.5	64.7	89.0
C_gc2′	0.35	23.47	-80.8	119.2	124.1	-74.7	C_sc3	0.44	15.26	-84.8	120.0	-61.6	178.3
C_gc3	1.17	5.95	86.5	-75.9	-45.3	-61.7	C_sc4	0.59	11.85	-90.2	125.3	-62.6	-91.8
C_gc4	1.69	2.45	-102.2	99.2	-71.3	-127.5	C_sc5	0.62	11.26	-85.2	121.0	-61.6	137.1
C_gc5	1.79	2.07	91.4	-112.7	64.2	158.5	C_sc6	0.64	10.89	-86.5	119.9	-62.1	-176.8
1d							**1d**						
C_gd1	0.00	43.00	80.5	-97.5	-171.8	78.4	C_sd1	0.00	36.67	-112.0	85.0	61.4	88.6
C_gd1′	0.01	42.46	-80.6	97.2	171.6	-78.7	C_sd2	0.27	23.25	-89.1	113.5	-60.6	173.7
C_gd2	1.35	4.39	81.0	-112.8	46.9	-115.0	C_sd3	0.31	21.73	-85.5	88.1	63.1	89.4
C_gd3	1.39	4.15	-89.2	73.8	50.5	76.7	C_sd4	0.41	18.35	-93.0	112.0	-63.2	-174.3
C_gd4	1.47	3.61	-84.6	112.2	-47.0	114.2	-	-	-	-	-	-	-
C_gd5	1.71	2.39	-96.3	106.7	-65.9	-154.3	-	-	-	-	-	-	-

[a] All energy values are in kcal/mol. [b] Vales relative the most stable conformer. [c] Boltzmann populations relative to the lowest Gibbs energy conformer. [d] Dihedral definitions for **1a**-**1d** see Fig. 1. The absolute Gibbs energy values for the lowest energy conformers are given in Table 2.

Table 2

Absolute values (hartrees) of G_{gas} and G_{sol} for the conformers of **1a**-**1d** presenting the lowest Gibbs energy (C_ga1-C_gd1 and C_sa1-C_sd1).

compound	G_{gas}	G_{soln}
1a	-996.112861	-989.872149
1b	-1035.420662	-1028.896868
1c	-1035.429171	-1028.910397
1d	-1074.738495	-1067.935904

Table 3

Distances (*d* and *D* in Å) and angular parameters (θ and φ in °) for the minimum energy conformers of **1a-1d**.[a]

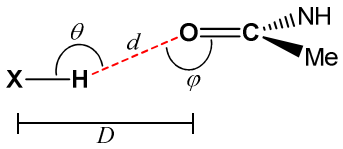

	gas phase					aqueous solution			
	d	*D*	θ	φ		*d*	*D*	θ	φ
1a					**1a**				
C_ga1	2.17	3.32	132.51	109.69	C_sa1	2.27	3.30	132.05	105.84
C_ga1′	2.17	3.32	132.50	109.68	C_sa2	2.29	3.34	130.91	106.64
C_ga2	2.18	3.33	131.72	110.22	-	-	-	-	-
C_ga2′	2.18	3.33	131.70	110.21	-	-	-	-	-
1b					**1b**				
C_gb1	2.36	3.31	164.01	103.12	C_sb1	3.68	4.25	-[b]	-[b]
C_gb2	2.35	3.79	164.10	104.90	C_sb2	3.54	4.18	-[b]	-[b]
C_gb3	2.47	3.79	-[b]	-[b]	-				
C_gb3′	2.47	3.48	-[b]	-[b]	-				
1c					**1c**				
C_gc1	2.01	3.31	150.69	105.23	C_sc1	4.05	4.02	-[b]	-[b]
C_gc2	2.02	3.79	152.22	133.43	C_sc2	4.03	4.21	-[b]	-[b]
C_gc2′	2.02	3.79	152.15	133.40	C_sc3	5.00	4.71	-[b]	-[b]
C_gc3	2.95	3.48	-[b]	-[b]	C_sc4	5.71	4.89	-[b]	-[b]
C_gc4	6.18	5.46	-[b]	-[b]	C_sc5	4.03	4.21	-[b]	-[b]
C_gc5	5.10	5.62	-[b]	-[b]	C_sc6	5.12	4.77	-[b]	-[b]
1d					**1d**				
C_gd1	2.62	3.71	177.23	126.56	C_sd1	3.19	3.74	-[b]	-[b]
C_gd1′	2.62	3.71	178.97	126.68	C_sd2	4.69	5.07	-[b]	-[b]
C_gd2	2.64	3.69	-[b]	-[b]	C_sd3	3.25	3.73	-[b]	-[b]
C_gd3	2.58	3.49	-[b]	-[b]	C_sd4	5.12	5.28	-[b]	-[b]
C_gd3′	2.58	3.48	-[b]	-[b]	-	-	-	-	-
C_gd4	5.57	5.99	-[b]	-[b]	-	-	-	-	-

[a] According to geometric criteria, the hydrogen bonds in the generic molecule X−H···O (X = C, N) are determined by the following parameters: *d* = 1.5−3.2 Å, *D* = 2.5−4.0 Å, θ = 90−180°, φ = 100−260° [28-31].

[b] Electron lone pair direction of the acceptor carbonyl oxygen is deviated too severely from the hydrogen donor atom.

Table 4

Selected ^{1}H spectral data (δ in ppm) for **1a**-**1c** in $CDCl_3$ and DMSO-d_6 solutions.[a]

compond	solvent	N_1-H	N_1-Me	N_2-H	Me_{amide}
1a	$CDCl_3$	8.90	-	5.75	1.93
	DMSO-d_6	10.69	-	8.25	1.85
1b	$CDCl_3$	-	3.70	5.07	1.82
	DMSO-d_6	-	3.69	8.20	1.82
1c	$CDCl_3$	8.52	-	5.40	1.77
	DMSO-d_6	10.80	-	7.94	1.76

[a] The indole nitrogen atom is designated as N_1 and the amide nitrogen as N_2.

*2.2.3. Mapping of the solvated minimum energy conformers of **1a-1d***

The benefit of complementing pharmacophore mapping results with the information obtained about the predicted conformational preference for **1a**-**1d** in aqueous solution is to determine how well statistically significant conformers characterize the antagonist pharmacophore model. In order to check whether a chemical feature is present in a given conformer all sets of conformers of **1a**-**1d** were aligned with the agonist and antagonist hypotheses by a rigid fit procedure. An inspection of results showed that, in general, the two most stable conformers of **1a**-**1d**, namely *C*$_s$a1, *C*$_s$a2, *C*$_s$b1, *C*$_s$b2, *C*$_s$c1, *C*$_s$c2, and *C*$_s$d1, together with *C*$_s$d3, mapped reasonably well the antagonist hypothesis. Except for *C*$_s$a2, *C*$_s$c1 and *C*$_s$d1, the pharmacophore maps on all these conformers on two hydrogen-bond acceptor sites, one hydrogen-bond donor site and two aromatic hydrophobic regions, whereas these conformers either do not map at all or map fewer of the features of the agonist model (Fig. 7). The fit scores are presented in Table S4 in the Supplementary.

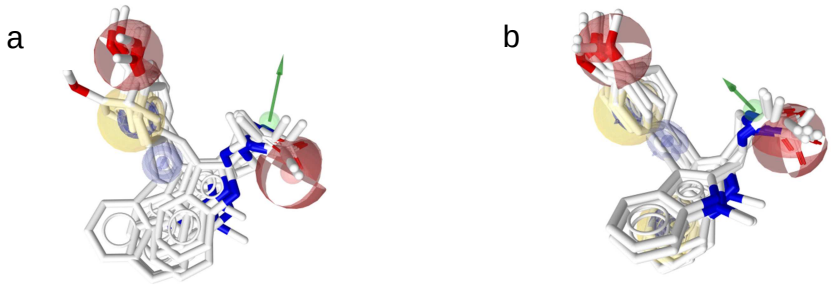

Fig. 7. Alignment of the lower energy conformers of **1a-1d** with the chemical features of (a) agonist model (b) antagonist model.

2.3. Synthesis of 2-(N-acylaminoalkyl)indole derivatives

In sharp contrast with the number of 3-(*N*-acylaminoethyl)indoles identified as melatoninergic ligands, those examples related with their regioisomeres in which the 2-aminoethyl appendage is attached at the C2 indole core are very scarce [33-35]. The synthesis of 2-(*N*-acylaminoalkyl)indoles **1a-1d** was started with the study of the electrophilic benzylation of electron deficient indole **2** (Scheme 1) [36]. Thus, the benzylation of **2** with *p*MeOBnCl conducted under various conditions, from 10 to 70 °C and for 45 min up to 90 h reaction time, showed that the best result was observed when the reaction was performed with 2.25 equiv of *p*MeOBnCl in glacial acetic acid at 60 °C for 1.5 h. Under these conditions the *p*MeOBn group was introduced at the C3 and C5-position of the indole nucleus to afford the mono- and di-benzylated compounds **3a** and **3b** in 2:1 ratio and in a global yield of 62%. In every experiment, we found that **2** was never fully consumed and in no case was *N*-substitution observed [37]. It is worthy to mention that the ease of displacement of the halide depended strongly on the electrophilicity; under the conditions analyzed no reaction occurred with BnCl. Single crystals of **3a** and **3b** were obtained, the X-ray data showed that the carbonyl group and the hydrogen atom at *N*-1 are *syn* oriented with respect to one another, and the dihedral angle between the carbonyl group and the N(1)-C(2) bond is about 0° in both compounds favoring conjugative interactions (Fig. 8).

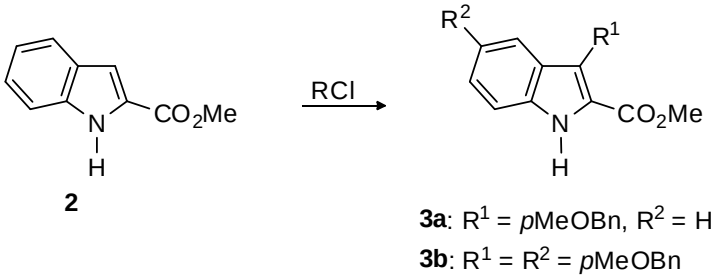

Scheme 1. Preparation of 3-substituted- and 3,5-disubstituted 2-carbometoxyindoles **3a** and **3b**. Reagents and conditions: (*a*) *p*-MeOBnCl, glacial AcOH, room temperature, 1.5 h.

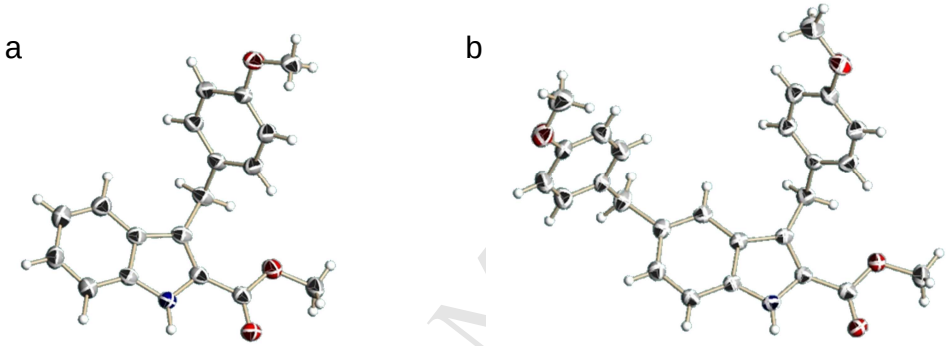

Fig. 8. X-ray structures of **3a** (a) and **3b** (b); ellipsoids drawn at the 30% probability level.

The multistep transformation of **3a** to **1a-1c** (Scheme 2) was conducted following a slightly modified literature procedure [38]. Briefly, ester **3a** was saponified and the carboxilic acid **4** was converted to the carboxamide **5** by reaction with oxalyl chloride and then with ammonium hydroxide in 88% combined yield. Reduction of amide **5** with $LiAlH_4$ afforded the corresponding unstable amine **6**. The 2-(*N*-acylaminomethyl)indole derivative **1a** was prepared by *N*-acylation of **6** with acetic anhydride in 62% global yield from **5**. Treatment of **1a** with KOH in DMSO, followed by MeI provided the N_1,N_2-dimethylated product **7**. Selective N_1-methylation of **1a** was carried out with MeI in the presence of a weaker base, Cs_2CO_3, to give **1b** in 62% isolated yield. Alternatively, the carboxilic acid **4** was converted to the *N*,*N*-diethylcarboxamide **8** by reaction with dicyclohexylcarbodiimide (DCC) and then with diethylamine, albeit in only in 20% yield. Reduction of amide **8** with $LiAlH_4$ gave the *N*,*N*-diethylmethanamine **9** in 49% yield. Reaction of the ammonium salt of **9** with potassium cyanide provided the nitrile **10** in 36% yield. In solution **10** was

unstable, decomposition occurs noticeably for 1 day, whereas upon standing neat at room temperature **10** crystallized as reddish needles. Structures of compounds **8** and **10** from single crystal X-ray diffraction studies are shown in Fig. 9. Treatment of **10** with MeI using Cs_2CO_3 as a base furnished the *N*-methylated product **11a** in mixture with the *C*-monomethylated and *C*,*N*-dimethylated products **11b** and **11c** in 5:2:4 ratio, respectively, and in a global yield of 55%. Finally, the 2-(*N*-acylaminoethyl)indole derivative **1c** was prepared by hydrogenation of **10** over Raney nickel and concomitant *N*-acylation with acetic anhydride in 65% yield of the crude product. It was observed that compound **1c** was spontaneously oxidized in air. Indeed, mass spectrometric and NMR analyses revealed that upon storage, neat **1c** degraded in the presence of oxygen, allowing cleanly an entry to the 2,2-disubstituted indoline-3-one derivative **12** (Scheme 3). Under these circumstances, the *N*-methyl derivative **1d** could not be obtained from unstable **1c**.

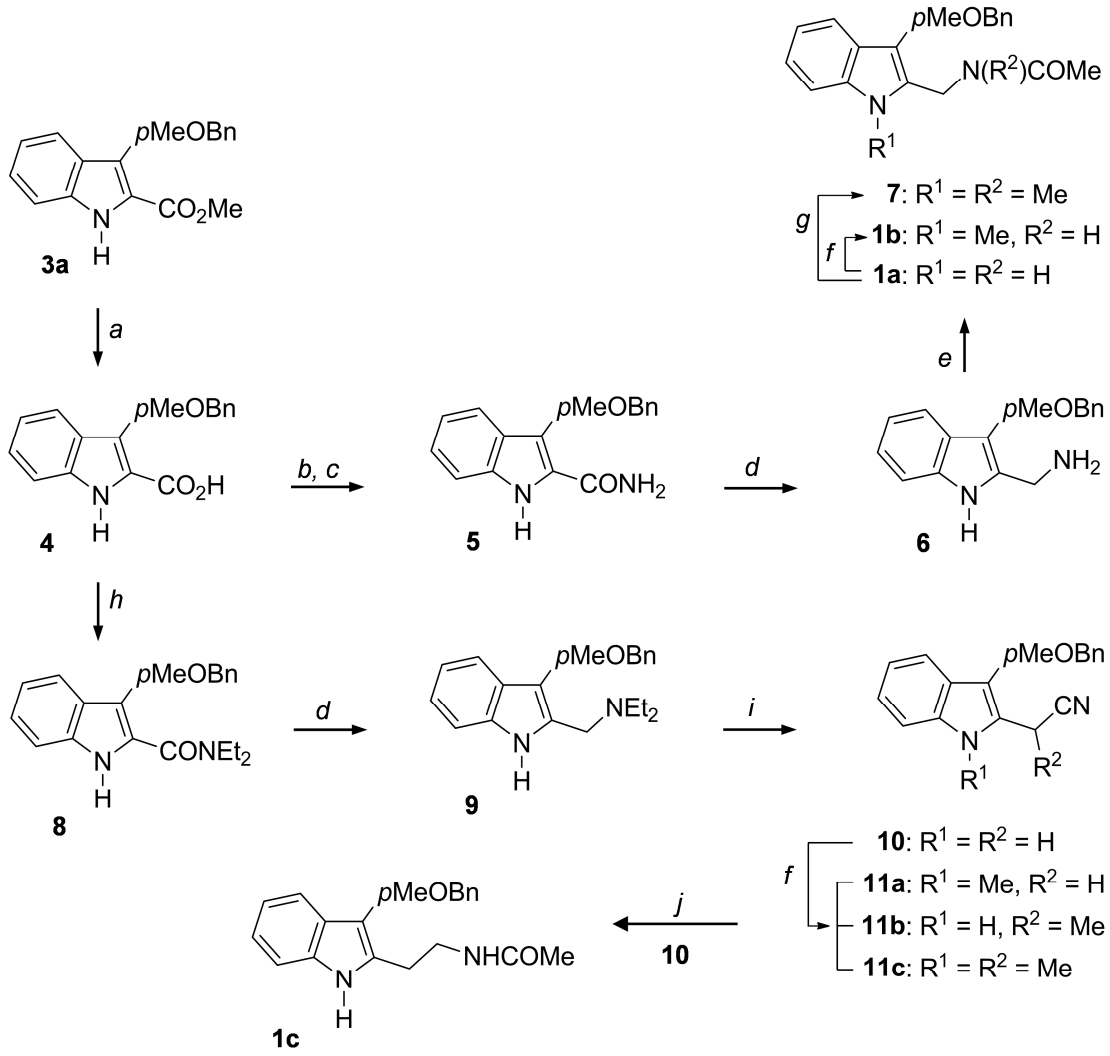

Scheme 2. Synthesis of 2-(*N*-acylaminoalkyl)indoles **1a**-**1d**. Reagents and conditions: (*a*) 20% aq NaOH, MeOH, THF, reflux, 6 h; (*b*) oxalyl chloride, CH_2Cl_2, DMF, rt, 4.5 h; (*c*) NH_4OH, rt, 18 h; (*d*) $LiAlH_4$, THF, reflux, 6 h; (*e*) $(Ac)_2O$, NEt_3, THF, rt, 6 h; (*f*) Cs_2CO_3, DMF, MeI, rt, 24 h; (*g*) KOH, DMSO, MeI, reflux, 4 h; (*h*) DMPA, DCC, $CHCl_3$, Et_2NH, reflux, 24 h; (*i*) MeI, MeOH, rt, 2 h, then 40% aq KCN, reflux, 1.5 h (*j*) H_2, Raney-Ni W2, Ac_2O, 3 atm, rt, 5 h.

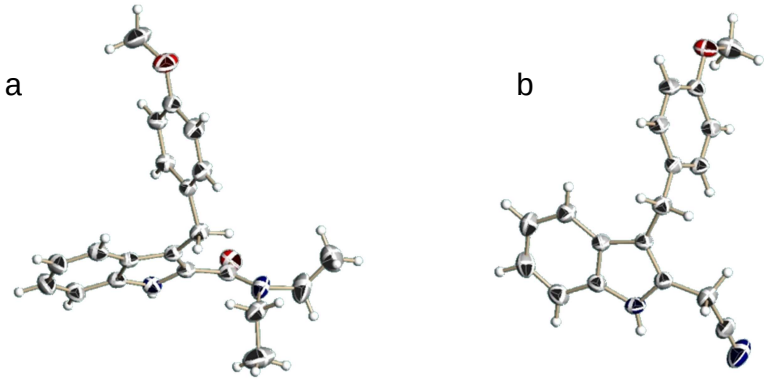

Fig. 9. X-ray structures of **8** (a) and **10** (b); ellipsoids drawn at the 30% probability level.

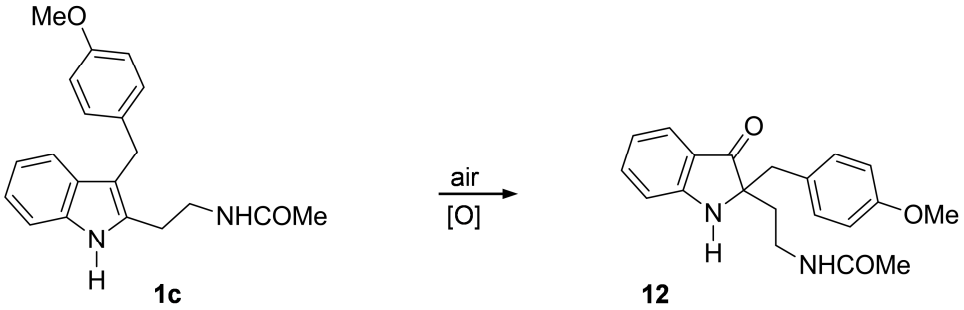

Scheme 3. Formation of 2,2-disubstituted indoline-3-one derivative **12**.

3. Conclusions

Pharmacophoric models for melatoninergic agonist and antagonist ligands were generated and used these models for the virtual screening of **1a-1d** compounds. Analysis of the resulting structural alignment showed the best-fit with the antagonist eight-point pharmacophore model, largely because the hydrophobic benzyl center has no comparable constituent in the agonist model. Compounds **1c** and **1d** exhibited superior structural overlay with the antagonist model over its lower homologues **1a** and **1b**. In addition, theoretical conformational analysis in the gas phase at the B3LYP/6-31G+(d,p) level hypothesized intramolecular H-bonding as essential factor in determining stable conformations for **1a-1d**. These results diverge with those in the aqueous phase where

conformational changes do not permit such H-bond. In addition, statistically significant conformers calculated at the same level using PCM solvation model matched the antagonist pharmacophore mapping. Although this initial study suggests that indoles **1a**-**1d** bearing an amidoalkyl side chain at C-2 and a *p*-methoxybenzyl substructure at C-3 are expected to show activity as antagonist melatoninergic ligands, their relative stability, which decreases in the order **1b** > **1a** > **1c**, discourages biological studies.

4. Experimental section

4.1 Computational Part

Automated pharmacophoric studies were carried out using the LigandScout 3.12 program available from Inte:Ligand GmbH (http://www.inteligand.com/). The three-dimensional structure of the molecules **1a**-**1d** was built using ChemBioOffice 12.0 [39]. All computational optimizations were carried out by using the Gaussian 03 or 09 program package [26,27]. A Monte Carlo random conformational search with the MMFF94 force-field minimization [40] was applied for every compound to give 14-16 conformers in the first 3 kcal/mol. The calculations were carried out using the Spartan 04 molecular modeling software program [41,42]. Geometry optimizations for gas-phase conformers were performed at the DFT level by applying the B3LYP functional [43] and 6-31G+(d,p) basis set [44]. A frequency analysis was carried out in each case to ascertain that a real minimum had been obtained (i.e., no imaginary vibrational frequencies). To simulate physiological conditions, the conformational search was performed in the presence of an aqueous environment using the free energy perturbation MMFFaq method implemented in Monte Carlo simulations. The calculations were carried out using the Spartan 14 software [45]. Geometry optimizations were performed at the DFT level by applying the B3LYP functional and 6-31G+(d,p) basis set using Tomasi's polarizable continuum model (PCM) [46-48] and the dielectric constant of water at 298.15 K (ε = 78.4).

4.2 Chemistry

All reagent-grade chemicals were purchased from Sigma-Aldrich Co. and were used as received. Melting points were determined on an electrothermal instrument and are uncorrected. IR spectra were obtained in chloroform. Low-resolution mass spectra were conducted on a Varian CP 3800 GC spectrometer equipped with a selective mass Varian Saturn 2000 detector. MS analyses were obtained in the electron impact (EI) mode at an ionizing voltage of 70 eV. High-resolution mass spectra (HRMS) were recorded on an Agilent LCTOF spectrometer at the UCR Mass Spectrometry Facility, University of California, Riverside, CA and on a Waters Synapt G2 HDMS spectrometer at the Central Analytical Laboratory, Department of Chemistry and Biochemistry, University of Colorado at Boulder. ^{1}H and ^{13}C NMR spectra were recorded on Varian Mercury spectrometers (300 MHz for ^{1}H and 75 MHz for ^{13}C) using $CDCl_3$ as a solvent unless indicated otherwise. Chemical shifts are given in ppm (δ) and are referenced to TMS as internal standard. *J* values are quoted in Hertz, with the normal abbreviations (s, singlet; d, doublet; t, triplet; q, quartet; br, broad; m, multiplet). All structural assignments were supported by gHMBC, gHSQC, and NOESY. Analytical thin-layer chromatography (TLC) was performed on silica gel 60 F254 coated aluminum sheets (0.25 mm thickness) with a fluorescent indicator. Visualization was accomplished with UV light (254 nm). Flash chromatography was performed on silica gel 60 (230-400 mesh).

*4.2.1. Methyl 3-(4-methoxybenzyl)-1H-indole-2-carboxylate (**3a**) and methyl 3,5-bis(4-methoxybenzyl)-1H-indole-2-carboxylate (**3b**).* A glacial acetic acid suspension (16.5 M, 48 mL) of commercial available methyl 1*H*-indole-2-carboxylate (**2**) (2.98 g, 17.01 mmoL) was stirred at 60 °C until solution, then brought up to room temperature and *p*-MeOBnCl (2.25 mL, 16.5 mM) was added. After stirring at room temperature for 1.5 h, the reaction was diluted with water until cloudy (15 mL). The aqueous layer was extracted with EtOAc (3 x 30 mL), and the combined organic layers were washed with saturated aqueous $NaHCO_3$ and brine, dried over Na_2SO_4, and concentrated in vacuo to give a mixture of mono- and di-benzylated compounds **3a** and **3b** in 2:1 ratio, as determined by ^{1}H NMR. The mixture was separated by flash chromatography (hexane/EtOAc 4:1) to afford

successively **3a** (1.94 g, 7.0 mmol, 41% yield) and **3b** (0.99 g, 2.38 mmol, 21%). Recrystallization of **3a** or **3b** from hexane/EtOAc gave colorless crystals suitable for X-ray crystallography. For **3a**: Mp: 158-159 °C. R_f = 0.60 (hexane/EtOAc 7:3); ^{1}H NMR ($CDCl_3$) δ: 8.75 (br s, 1H, NH), 7.61 (dm, J = 8.2 Hz, 1H, H-4), 7.37 (dm, J = 8.2 Hz, 1H, H-7), 7.31 (ddd, J = 8.3, 6.7, 1.2 Hz, 1H, H-6), 7.19 (dm, J = 8.8 Hz, 2H, H*o*), 7.10 (ddd, J = 8.2, 6.7, 1.2 Hz, 1H, H-5), 6.77 (dm, J = 8.8 Hz, 2H, H*m*), 4.44 (s, 2H, CH_2) 3.94 (s, 3H, CO_2Me), 3.75 (s, 3H, OMe); ^{13}C NMR ($CDCl_3$) δ: 162.8 (C=O), 157.7 (C*p*), 136.1 (C-7a), 133.1 (C*i*), 129.3 (C*o*), 127.9 (C-3a), 125.6 (C-6), 123.3 (C-3), 123.2 (C-2), 121.2 (C-4), 120.2 (C-5), 113.7 (C*m*), 111.7 (C-7), 55.1 (OMe), 51.7 (CO_2Me), 29.6 (CH_2); IR ($CHCl_3$, cm^{-1}) ν_{max} = 3460, 3344, 1697; GC-MS (EI, 70 eV): *m*/*z* (%) = 295 (M^+, 87), 264 (100); HRMS: *m*/*z* calcd for $C_{18}H_{17}NO_3$ (M + H) 296.1282, found 296.1282. CCDC-1469876.

For **3b**: Mp: 164-166 °C R_f = 0.45 (hexane/EtOAc 7:3); ^{1}H NMR ($CDCl_3$) δ: 8.75 (br s, 1H, NH), 7.39 (m, 1H, H-4), 7.25 (dd, J = 8.5, 0.7 Hz, 1H, H-7), 7.16 (dm, J = 8.8 Hz, 2H, H*o*), 7.12 (d, J = 1.8 Hz, 1H, H-6), 7.08 (dm, J = 8.8 Hz, 2H, H*o*'), 6.81 (dm, J = 8.8 Hz, 2H, H*m*'), 6.76 (dm, J = 8.8 Hz, 2H, H*m*'), 4.39 (s, 2H, CH_2), 3.96 (s, 2H, CH_2'), 3.91 (s, 3H, CO_2Me), 3.77 (s, 3H, OMe'), 3.75 (s, 3H, OMe); ^{13}C NMR ($CDCl_3$) δ: 162.7 (CO), 157.9 (C*p*'), 157.7 (C*p*), 134.7 (C-7a), 133.8 (C*i*'), 133.5 (C-5), 133.1 (C*i*), 129.8 (C*o*'), 129.3 (C*o*), 128.1. (C-3a), 127.3 (C-6), 123.3 (C-3), 123.2 (C-2), 120.6 (C-4), 113.8 (C*m*'), 113.7 (C*m*), 111.8 (C-7), 55.2 (OMe'), 55.2(OMe), 51.7 (CO_2Me), 41.1 (CH_2'), 29.6 (CH_2); IR ($CHCl_3$, cm^{-1}) ν_{max} = 3455, 3351, 1695; GC-MS (EI, 70 eV): m/z (%) = 295 (56), 281 (19), 264(100), 221(30); HRMS: *m*/*z* calcd for $C_{26}H_{25}NO_4$ (M + Na) 438.1681, found 438.1673. CCDC-1469877.

*4.2.2. 3-(4-Methoxybenzyl)-1H-indole-2-carboxylic acid (**4**).* To a stirred and cooled (0 °C) suspension of **3a** (0.3 g, 1.02 mmol) in MeOH (6 mL) was added 20% aqueous NaOH (1.2 mL). The ice bath was removed, and the reaction was heated at reflux for 6 h. The reaction mixture was cooled (0 °C) and 1 M HCl was added with stirring to adjust the pH to about 3-4. The solids were filtered off, washed with water and dried at 50 °C overnight to give **4** as a white solid (0.27 g, 0.97 mmol, 95%). Mp: 242-243 °C. R_f = 0.18 (hexane/EtOAc 7:3). ^{1}H NMR (AcOD-d_4) δ: 7.61 (br d, J = 8.2 Hz, 1H, H-4), 7.44 (br d, J = 8.2 Hz, 1H, H-7), 7.28 (ddd, J = 8.2, 7.0, 1.2 Hz , H-6), 7.19 (dm, J = 8.8 Hz, 2H, H*o*), 7.05 (ddd, J = 8.2, 7.0,

1.2 Hz, 1H, H-5), 6.77 (dm, *J* = 8.8 Hz, 2H, H*m*), 4.46 (s, 2H, CH_2) 3.71 (s, 3H, OMe); ^{13}C NMR (AcOD-d_4) δ: 167.8 (CO), 158.8 (C*p*), 138.3 (C-7a), 134.2 (C*i*), 130.2 (C*o*), 128.7 (C-3a), 126.8 (C-6), 125.9 (C-3), 123.4 (C-2), 122.1 (C-4), 121.5 (C-5), 114.6 (C*m*), 113.2 (C-7), 55.4 (OMe), 30.3 (CH_2); IR ($CHCl_3$, cm^{-1}) ν_{max} = 3080, 1712; GC-MS (EI, 70 eV): *m*/*z* (%) = 121 (100). HRMS: *m*/*z* calcd for $C_{17}H_{15}NO_3$ (M - H) 280.0979, found 280.0987.

*4.2.3. 3-(4-Methoxybenzyl)-1H-indole-2-carboxamide (**5**)*. To a suspension of **4** (273 mg, 0.97 mmol) in CH_2Cl_2 (6 mL) and DMF (0.02 mL) was added dropwise oxalyl chloride (0.2 mL, 2.35 mmol) and the mixture was allowed to stir for 4.5 h at room temperature. The reaction mixture was cooled (0 °C) and concentrated aqueous NH_4OH (1.05 mL) was added by portions. The ice bath was removed, and the reaction was stirred at room temperature for 18 h. The solids were filtered off, washed with water, dissolved in EtOAc, dried over Na_2SO_4, and concentrated in vacuo. The resulting yellowish solid was purified by crystallization (CH_2Cl_2/hexane) to give **5** (250 mg, 0.89 mmol, 93%) as colorless needles. Mp: 155-156 °C (CH_2Cl_2/hexane) (lit. [49] 150-152 °C). R_f = 0.37 (hexane/EtOAc 3:7); ^{1}H NMR ($CDCl_3$) δ: 9.55 (br s, 1H, NH), 7.65 (dm, *J* = 8.1, Hz, 1H, H-4), 7.45 (dm, *J* = 8.2 Hz, 1H, H-7), 7.32 (ddd, *J* = 8.2, 6.9, 1.2 Hz, 1H, H-6), 7.15 (ddd, *J* = 8.1, 6.9, 1.0 Hz, 1H, H-5), 7.11 (dm, *J* = 8.8 Hz, 2H, H*o*), 6.82 (dm, *J* = 8.8 Hz, 2H, H*m*), 5.87 (br s, 2H, NH_2), 4.36 (br s, 2H, CH_2), 3.75 (s, 3H, OMe); ^{13}C NMR ($CDCl_3$) δ: 163.5 (CO), 158.5 (C*p*), 135.4 (C-7a), 131.0 (C*i*), 129.0 (C*o*), 128.9 (C-3a), 127.2 (C-2), 125.2 (C-6), 120.4 (C-5), 120.3 (C-4), 116.2 (C-3), 114.5 (C*m*), 111.8 (C-7), 55.3 (OMe), 29.3 (CH_2); IR ($CHCl_3$, cm^{-1}) ν_{max} = 3493, 3445, 3384, 1659; GC-MS (EI, 70 eV): *m*/*z* (%) = 280 (M^+, 8), 263 (100), 249 (18), 220 (26). HRMS *m*/*z* calcd for $C_{17}H_{16}N_2O_2$ (M + H) 281.1285, found 281.1291.

*4.2.4. (3-(4-Methoxybenzyl)-1H-indol-2-yl)methanamine (**6**)*. In a dry flask, under Ar, a solution of **5** (424 mg, 1.51 mmol) in anhydrous THF (10 mL) was added dropwise to a suspension of $LiAlH_4$ (424 mg, 11.2 mmol) in anhydrous THF (10 mL). The mixture was stirred at reflux during 20 h. The reaction was cooled (0 °C), quenched with water (8 mL) and filtered over Celite. Following concentration, the residue was partitioned between CH_2Cl_2 (30 mL) and water (15 mL). The aqueous layer was extracted with CH_2Cl_2 (2 x 15

mL), and the combined organic layers were washed with brine, dried over Na_2SO_4, and concentrated in vacuo. The reddish oil residue was purified by flash chromatography (CH_2Cl_2/MeOH 9:1) to give **6** (321 mg, 1.21 mmol, 80%) as an unstable yellowish oil, experiencing decomposition even after short NMR acquisition times. R_f = 0.16 (CH_2Cl_2/MeOH 9:1); ^{1}H NMR ($CDCl_3$) δ: 8.63 (br s, 1H, NH), 7.42 (br d, *J* = 7.6 Hz, 1H, H-4), 7.32 (br d, *J* = 7.6 Hz, 1H, H-7), 7.14 (br dd, *J* = 7.0, 7.0 Hz, 1H, H-6), 7.10 (dm, *J* = 8.8 Hz, 2H, H*o*), 7.04 (br dd, *J* = 7.6, 7.6 Hz, 1H, H-5), 6.76 (dm, *J* = 8.8 Hz, 2H, H*m*), 4.01 (s, 2H, CH_2Ph), 3.98 (s, 2H, CH_2N) 3.74 (s, 3H, OMe), 1.94 (br s, 2H, NH_2); ^{13}C NMR ($CDCl_3$) δ: 157.7 (C*p*), 135.3 (C-7a), 134.7 (C-2), 133.6 (C*i*), 129.0 (C*o*), 128.6 (C-3a), 121.6 (C-6), 119.2 (C-5), 118.7 (C-4), 113.7 (C*m*), 110.7 (C-7 and C-3), 55.2 (OMe), 37.1 (CH_2N), 28.9 (CH_2Ph); IR ($CHCl_3$, cm^{-1}) ν_{max} = 3456, 3363; GC-MS (EI, 70 eV): *m*/*z* (%) = 266 (M^+, 1), 248 (100), 233 (24), 218 (36). HRMS: *m*/*z* calcd for $C_{17}H_{18}N_2O$ (M + Na) 289.1317, found 289.1317.

*4.2.5. N-((3-(4-Methoxybenzyl)-1H-indol-2-yl)methyl)acetamide (**1a**)*. To a solution of amine **6** (0.152g, 0.57 mmol) in a mixture of THF (3 mL) and triethylamine (0.1 mL, 0.8 mmol) was added acetic anhydride (0.075mL, 0.8 mmol). The mixture was stirred at room temperature for 6 h until disappearance of starting material (TLC). The resulting solution was concentrated in vacuo and the residue was taken up in EtOAc (25 mL). The organic layer was washed with saturated aqueous $NaHCO_3$ and brine, dried over Na_2SO_4, and concentrated in vacuo. The oil residue was purified by flash chromatography (hexane/EtOAc 3:2) to give **1a** (135 mg, 0.44 mmol, 77%) as an unstable yellowish oil. R_f = 0.22 (37 (hexane/EtOAc 3:7); ^{1}H NMR ($CDCl_3$) δ: 8.90 (br s, 1H, NH), 7.46 (br d, *J* = 7.6 Hz, 1H, H-4), 7.31 (br d, *J* = 8.2 Hz, 1H, H-7), 7.16 (ddd, *J* = 7.7, 7.7,1.2 Hz, 1H, H-6), 7.10 (dm, *J* = 8.8 Hz, 2H, H*o*), 7.05 (ddd *J* = 7.7, 7.7, 1.2 Hz, 1H, H-5), 6.80 (dm, *J* = 8.8 Hz, 2H, H*m*), 5.75 (br t, *J* = 5.9 Hz, 1H, NHCO), 4.39 (d, *J* = 5.9 Hz, 2H, CH_2N), 4.05 (br s, 2H, CH_2Ph), 3.75 (s, 3H, OMe), 1.93 (s, 3H, COMe); ^{13}C NMR ($CDCl_3$) δ: 171.5 (CO), 157.8 (C*p*), 135.4 (C-7a), 133.7 (C*i*), 132.7 (C-2), 129.1 (C*o*), 127.8 (C-3a), 122.1 (C-6), 119.3 (C-5), 118.9 (C-4), 113.8 (C*m*), 111.7 (C-3), 111.0 (C-7), 55.2 (OMe), 35.1 (CH_2NH), 28.9 (CH_2Ph), 23.0 (CO<u>Me</u>); ^{1}H NMR (DMSO-d_6) δ: 10.69 (br s, 1H, NH), 8.25 (br t, *J* = 5.3 Hz, 1H, NHCO), 7.30 (br d, *J* = 7.6 Hz, 1H, H-4), 7.28 (br d, *J* = 8.2 Hz, 1H,

H-7), 7.12 (dm, *J* = 8.8 Hz, 2H, H*o*), 6.98 (ddd, *J* = 8.2, 7.0, 1.2 Hz, 1H, H-6), 6.85 (ddd *J* = 7.6, 7.0, 1.2 Hz, 1H, H-5), 6.76 (dm, *J* = 8.8 Hz, 2H, H*m*), 4.41 (d, *J* = 5.8 Hz, 2H, CH_2N), 3.94 (s, 2H, CH_2Ph), 3.68 (s, 3H, OMe), 1.85 (s, 3H, COMe); ^{13}C NMR (DMSO-d_6) δ: 169.2 (CO), 157.2 (C*p*), 135.4 (C-7a), 133.7 (C*i*), 132.7 (C-2), 129.1 (C*o*), 127.6 (C-3a), 120.7 (C-6), 118.4 (C-5), 118.3 (C-4), 113.5 (C*m*), 111.0 (C-7), 110.7 (C-3), 54.9 (OMe), 34.1 (CH_2N), 28.5 (CH_2Ph), 22.5 (CO<u>Me</u>); IR ($CHCl_3$, cm^{-1}) ν_{max} = 3441, 1692, 1665; GC-MS (EI, 70 eV): *m*/*z* (%) = 308 (M^+, 25), 248 (72), 237 (100), 219 (23).

*4.2.6. N-((3-(4-methoxybenzyl)-1-methyl-1H-indol-2-yl)methyl)acetamide (**1b**)*. To a stirred suspension of amide **1a** (120 mg, 0.37 mmol) and Cs_2CO_3 (192 mg, 0.58 mmol) in DMF (2 mL) was added MeI (0.1 mL, 1.8 mmol). After stirring at room temperature for 72 h, the reaction was quenched with water (20 mL). The aqueous layer was extracted with EtOAc (3 x 30 mL), and the combined organic layers were washed with brine (20 mL), dried over Na_2SO_4, and concentrated in vacuo. The oil residue was purified by flash chromatography (hexane/EtOAc 1:1 to give **1b** (60 mg, 0.19 mmol, 62%) as colorless solid. Mp: 170-171 °C. R_f = 0.22 (hexane/EtOAc 3:7); ^1H NMR ($CDCl_3$) δ: 7.54 (br d, *J* = 7.6 Hz, 1H, H-4), 7.28 (br d, *J* = 8.2 Hz, 1H, H-7), 7.22 (ddd, *J* = 8.2, 7.0, 1.2 Hz, 1H, H-6), 7.11 (dm, *J* = 8.8 Hz, 2H, H*o*), 7.10 (ddd *J* = 7.6, 7.0, 1.2 Hz, 1H, H-5), 6.80 (dm, *J* = 8.8 Hz, 2H, H*m*), 5.07 (br d, *J* = 5.3 Hz, 1H, NH), 4.57 (d, *J* = 5.3 Hz, 2H, CH_2N), 4.08 (br s, 2H, CH_2Ph), 3.75 (s, 3H, OMe), 3.70 (s, 3H, NMe), 1.82(s, 3H, COMe); ^{13}C NMR ($CDCl_3$) δ: 169.3 (CO), 157.8 (C*p*), 136.8 (C-7a), 134.0 (C*i*), 132.5 (C-2), 129.1 (C*o*), 127.4 (C-3a), 122.1 (C-6), 119.3 (C-5), 118.9 (C-4), 113.9 (C*m*), 113.5 (C-3), 109.2 (C-7), 55.2 (OMe), 33.2 (CH_2N), 29.6 (NMe), 29.1 (CH_2Ph), 23.0 (CO<u>Me</u>); ^1H NMR (DMSO-d_6) δ: 8.20 (br t, *J* = 5.1 Hz, 1H, NHCO), 7.37 (dm, *J* = 8.3 Hz, 1H, H-7), 7.35 (dm, *J* = 7.6 Hz, 1H, H-4), 7.18 (dm, *J* = 8.7 Hz, 2H, H*o*), 7.09 (ddd, *J* = 8.2, 7.0, 1.3 Hz, 1H, H-6), 6.92 (ddd, *J* = 8.0, 7.0, 1.0 Hz, 1H, H-5), 6.77 (dm, *J* = 8.8 Hz, 2H, H*m*), 4.48 (d, *J* = 5.1 Hz, CH_2N), 4.02 (br s, 2H, CH_2Ph), 3.69 (s, 3H, NMe) 3.66 (s, 3H, OMe) 1.82 (s, 3H, COMe); ^{13}C NMR (DMSO-d_6) δ: 168.4 (CO), 157.2 (C*p*), 136.6 (C-7a), 133.7 (C*i*), 133.6 (C-2), 129.1 (C*o*), 126.8 (C-3a), 121.2 (C-6), 118.7 (C-4), 118.6 (C-5), 113.5 (C*m*), 112.1 (C-3), 109.3 (C-7), 54.9 (OMe), 32.2 (CH_2N), 29.6 (NMe), 28.8 (CH_2Ph), 22.4 (CO<u>Me</u>); IR ($CHCl_3$, cm^{-1}) ν_{max} = 3434, 1666;

GC-MS (EI, 70 eV): *m*/*z* (%) = 322 (M^+, 5), 262 (55), 251 (100), 233 (18). HRMS: *m*/*z* calcd for $C_{20}H_{22}N_2O_2$ (M + Na) 345.1579, found 345.1580.

*4.2.7. N-((3-(4-Methoxybenzyl)-1-methyl-1H-indol-2-yl)methyl)-N-methylacetamide (**7**).* To a solution of amide **1a** (120 mg, 0.37 mmol) in DMSO (2 mL) was added KOH (90 mg, 1.6 mmol). The mixture was stirred at room temperature for 1 h, and MeI (0.1 mL, 1.8 mmol) was added. After reacting for further for 4 h in the same conditions, the reaction was quenched with water (20 mL). The aqueous layer was extracted with EtOAc (3 x 30 mL), and the combined organic layers were washed with brine (20 mL), dried over Na_2SO_4, and concentrated in vacuo. The oil residue was purified by flash chromatography (hexane/EtOAc 1:1) to give **7** (60 mg, 0.18 mmol, 46%) as yellowish solid. Mp: 89-90 °C. R_f = 0.22 (hexane/EtOAc 3:7); ^{1}H NMR ($CDCl_3$) δ: 7.46 (br d, *J* = 7.6 Hz, 1H, H-4), 7.30 (br d, *J* = 8.2 Hz, 1H, H-7), 7.24 (ddd, *J* = 8.2, 6.4, 1.2 Hz, 1H, H-6), 7.09 (dm, *J* = 8.8 Hz, 2H, H*o*), 7.07 (ddd *J* = 7.6, 6.4, 1.2 Hz, 1H, H-5), 6.75 (dm, *J* =8.8 Hz, 2H, H*m*), 4.83 (br s, 2H, CH_2N), 4.12 (br s, 2H, CH_2Ph), 3.75 (s, 3H, OMe), 3.66 (s, 3H, NMe), 2.62 (s, 3H, NMeCO), 2.08 (s, 3H, COMe); ^{13}C NMR ($CDCl_3$) δ: 170.4 (CO), 157.7 (C*p*), 137.2 (C-7a), 133.3 (C*i*), 131.4 (C-2), 129.0 (C*o*), 127.5 (C-3a), 121.9 (C-6), 119.2 (C-5), 119.1 (C-4), 114.2 (C-3), 113.7 (C*m*), 109.0 (C-7), 55.2 (OMe), 39.0 (CH_2N), 33.7 (N<u>Me</u>CO), 29.6 (NMe), 29.1 (CH_2Ph), 21.9 (CO<u>Me</u>); ^{1}H NMR (DMSO-d_6) δ: 7.35 (br d, overlapped, 2H, H-4, H-7), 7.11 (ddd, *J* = 8.2, 6.5,1.2 Hz, 1H, H-6), 7.08 (dm, *J* = 8.8 Hz, 2H, H*o*), 6.94 (dd *J* = 7.5, 6.6 Hz, 1H, H-5), 6.76 (dm, *J* =8.8 Hz, 2H, H*m*), 4.78 (br s, 2H, CH_2N), 4.04 (br s, 2H, CH_2Ph), 3.65 (s, 3H, OMe), 3.60 (s, 3H, NMe), 2.62 (s, 3H, NMeCO), 2.01(s, 3H, COMe); ^{13}C NMR (DMSO-d_6) δ: 169.7 (CO), 157.2 (C*p*), 136.8 (C-7a), 133.5 (C*i*), 131.9 (C-2), 129.0 (C*o*), 126.9 (C-3a), 121.4 (C-6), 118.8 (C-4), 118.7 (C-5), 113.6 (C-3), 113.5 (C*m*), 109.4 (C-7), 54.9 (OMe), 38.2 (CH_2N), 33.5 (N<u>Me</u>CO), 30.0 (NMe), 28.4 (CH_2Ph), 21.7 (CO<u>Me</u>); IR ($CHCl_3$, cm^{-1}) ν_{max} = 1629; GC-MS (EI, 70 eV): *m*/*z* (%) = 336 (M^+, 0.3), 263 (95), 251 (100), 233 (25). HRMS: *m*/*z* calcd for $C_{21}H_{24}N_2O_2$ (M + Na) 359.1736, found 359.1737.

*4.2.8. N,N-Diethyl-3-(4-methoxybenzyl)-1H-indole-2-carboxamide (**8**).* To a solution of **4** (1.0 g, 3.6 mmol) in $CHCl_3$ (60 mL) was added successively 4-(dimethylamino)pyridine

(DMAP) (549 mg, 4.5 mmol) and dicyclohexylcarbodiimide (DCC) (618 mg, 3.0 mmol) at room temperature, and Et_2NH (300 μL) was then added dropwise. After stirring at reflux for 24 h, the reaction was quenched with brine (30 mL). The organic layer was separated, and the aqueous layer was extracted with $CHCl_3$ (2 x 10 mL). The combined organic extracts were dried over Na_2SO_4, and concentrated in vacuo. The residue was suspended in cool THF (30 mL), filtered, and the filtrate concentrated in vacuo. The oil residue was purified by flash chromatography (hexane/EtOAc 9:1 to 1:1 gradient) to give **8** (243 mg, 0.72 mmol, 20%) as colorless solid. Mp: 174-175 °C; R_f = 0.53 (hexane/EtOAc 1:1); ^{1}H NMR ($CDCl_3$) δ: 8.30 (br s, 1H, NH), 7.40 (dm, *J* = 8.1 Hz, 1H, H-4), 7.34 (dm, *J* = 8.1 Hz, 1H, H-7), 7.19 (ddd, *J* = 8.2, 7.0, 1.3 Hz, 1H, H-6), 7.15 (dm, *J* = 8.9 Hz, 2H, H*o*), 7.03 (ddd, *J* = 8.1, 7.0, 1.2 Hz, 1H, H-5), 6.77 (dm, *J* = 8.8 Hz, 2H, H*m*), 4.09 (s, 2H, CH_2Ph), 3.75 (s, 3H, OMe), 3.45 (q, *J* = 7.1 Hz, 4H, 2 NCH_2), 1.12 (t, *J* = 7.1 Hz, 6H, 2 Me); ^{13}C NMR ($CDCl_3$) δ: 165.2 (C=O), 157.8 (C*p*), 135.8 (C-7a), 132.4 (C*i*), 129.3 (C*o*), 128.9 (C-2), 127.5 (C-3a), 123.2 (C-6), 120.2 (C-4), 119.8 (C-5), 114.2 (C-3), 113.7 (C*m*), 111.5 (C-7), 55.2 (OMe), 41.0 (NCH_2), 29.9 (CH_2Ph), 13.6 (Me); IR ($CHCl_3$, cm^{-1}) ν_{max} = 3458, 3262, 1611; GC-MS (EI, 70 eV): *m*/*z* (%) = 336 (M^+, 3), 263 (100). HRMS: *m*/*z* calcd for $C_{21}H_{24}N_2O_2$ (M + H) 337.1911, found 337.1926. CCDC-1469878.

*4.2.9. N-Ethyl-N-((3-(4-methoxybenzyl)-1H-indol-2-yl)methyl)ethanamine (**9**).* In a dry flask, under Ar, a solution of **8** (300 mg, 0.9 mmol) in anhydrous THF (6 mL) was added dropwise to a suspension of $LiAlH_4$ (84 mg, 2.2 mmol) in anhydrous THF (2 mL), and the mixture was stirred at reflux during 4 h. After cooled (0 °C), the reaction was quenched with water (8 mL) and filtered over Celite. Following concentration, the residue was partitioned between CH_2Cl_2 (30 mL) and water (15 mL). The aqueous layer was extracted with EtOAc (2 x 15 mL), and the combined organic layers were washed with brine, dried over Na_2SO_4, and concentrated in vacuo. The oil residue was purified by crystallization (hexane/Et_2O) to give **9** (140 mg, 0.44 mmol, 49%) as pale yellow crystals. Mp: 113-116 °C; R_f = 0.47 (hexane/EtOAc 1:1); ^{1}H NMR ($CDCl_3$) δ: 8.54 (br s, 1H, NH), 7.39 (dm, *J* = 7.9 Hz, 1H, H-4), 7.30 (dm, *J* = 7.9 Hz, 1H, H-7), 7.12 (ddd, *J* = 8.1, 7.0, 1.3 Hz, 1H, H-6), 7.10 (dm, *J* = 8.8 Hz, 2H, H*o*), 7.00 (ddd, *J* = 7.8, 7.0, 1.2 Hz, H-5), 6.76 (dm, *J* = 8.7 Hz, 2H, H*m*), 4.03 (s, 2H, CH_2Ph), 3.73(s, 3H, OMe), 3.67 (s, 2H, CH_2N), 2.51 (q, *J* = 7.2 Hz,

4H, 2 C<u>H</u>$_2$CH$_3$), 1.00 (t, *J* = 7.2 Hz, 6H, 2 CH$_2$C<u>H</u>$_3$); ^{13}C NMR (CDCl$_3$) *δ*: 157.6 (C*p*), 135.3 (C-7a), 133.9 (C-2), 133.7 (C*i*), 129.1 (C*o*), 128.9 (C3a), 121.2 (C-6), 118.9 (C-5), 118.6 (C-4), 113.6 (C*m*), 111.3 (C-3), 110.5 (C-7), 55.2 (OMe), 48.9 (CH$_2$N), 47.0 (<u>C</u>H$_2$CH$_3$), 28.9 (CH$_2$Ph), 11.7 (CH$_2$<u>C</u>H$_3$); IR (CHCl$_3$, cm^{-1}) ν_{max} = 3447, 3349; GC-MS (EI, 70 eV): *m*/*z* (%) = 323 (M$^+$, 1), 249 (100), 219 (42).

*4.2.10. 2-(3-(4-Methoxybenzyl)-1H-indol-2-yl)acetonitrile (**10**)*. To a stirred and cooled (0 °C) solution of **9** (300 mg, 0.93 mmol) in MeOH (1.1 mL) was added MeI (145 μL, 2.3 mmol). The reaction was stirred at room temperature for 2 h, then 40% aqueous KCN (450 μL, 2.9 mmol) was added, and the mixture was refluxed for 1.5 h. The mixture was extracted with EtOAc (3 x 10 mL), and the combined organic layers were washed with brine, dried over Na$_2$SO$_4$, and concentrated in vacuo. The residue was purified by flash chromatography (hexane/EtOAc 7:3) to give **10** as an oil, which upon standing neat at room temperature crystallized as reddish needles (93 mg, 0.33 mmol, 36%). Mp: 120-122 °C; R_f = 0.38 (hexane/EtOAc 7:3); ^{1}H NMR (CDCl$_3$) *δ*: 8.17 (br s, 1H, NH), 7.45 (dm, *J* = 7.6 Hz, 1H, H-4), 7.33 (dm, *J* = 8.2 Hz, 1H, H-7), 7.20 (ddd, *J* = 8.2, 7.0, 1.2 Hz, 1H, H-6), 7.09 (dm, *J* = 8.8 Hz, 2H, H*o*), 7.09 (overlapped, 1H, H-5); 6.79 (dm, *J* = 8.8 Hz, 2H, H*m*), 4.01 (s, 2H, CH$_2$Ph), 3.74 (s, 3H, OMe), 3.70 (s, 2H, CH$_2$CN); ^{13}C NMR (CDCl$_3$) *δ*: 158.0 (C*p*), 135.7 (C-7a), 132.0 (C*i*), 129.1 (C*o*), 128.2 (C-3a), 122.8 (C-6), 122.1 (C-2), 120.1 (C-5), 119.1 (C-4), 116.4 (CN), 114.0 (C*m*), 113.6 (C-3), 110.9 (C-7), 55.2 (OMe), 29.0 (CH$_2$Ph), 15.6 (<u>C</u>H$_2$CN); IR (CHCl$_3$, cm^{-1}) ν_{max} = 3456, 3408, 2258; GC-MS (EI, 70 eV): *m*/*z* (%) = 276 (M$^+$, 100), 237 (15); HRMS: *m*/*z* calcd for C$_{18}$H$_{16}$N$_2$O (M - H) 275.1179, found 275.1182. CCDC-1469879.

*4.2.11. 2-(3-(4-Methoxybenzyl)-1-methyl-1H-indol-2-yl)acetonitrile (**11a**), 2-(3-(4-methoxybenzyl)-1H-indol-2-yl)propanenitrile (**11b**) and 2-(3-(4-methoxybenzyl)-1-methyl-1H-indol-2-yl)propanenitrile (**11c**)*. To a stirred suspension of nitrile **10** (120 mg, 0.44 mmol) and Cs$_2$CO$_3$ (225 mg, 1.4 mmol) in DMF (3 mL) was added MeI (120 μL, 1.9 mmol). After stirring at room temperature for 24 h, the reaction was quenched with water (20 mL). The aqueous layer was extracted with EtOAc (3 x 15 mL), and the combined organic layers were washed with brine (10 mL), dried over Na$_2$SO$_4$, and concentrated in

vacuo to give a mixture of mono- and dimethylated compounds **11a**, **11b**, and **11c** in ca. 5:2:4 ratio, respectively as determined by CG/MS. The mixture was separated by flash chromatography using hexane/CH_2Cl_2/EtOAc solvent mixture. Elution with 50:48:2 solvent mixture ratio gave successively **11c** (27 mg, 0.09 mmol, 20% yield), **11a** (30 mg, 0.1 mmol, 25% yield), and **11b** (12 mg, 0.04 mmol, 10% yield) as yellow oils. Further elution with 50:40:10 solvent mixture ratio yielded the starting material **10** (18 mg). For **11a**: R_f = 0.30 (hexane/CH_2Cl_2/EtOAc 50:48:2); ^{1}H NMR ($CDCl_3$) δ: 7.47 (dm, J = 7.6 Hz, 1H, H-4), 7.32 (dm, J = 8.2 Hz, 1H, H-7), 7.26 (overlapped, 1H, H-6), 7.11 (dm, J = 8.8 Hz, 2H, H*o*), 7.09 (overlapped, 1H, H-5); 6.80 (dm, J = 8.8 Hz, 2H, H*m*), 4.08 (s, 2H, CH_2Ph), 3.81 (s, 3H, NMe), 3.79 (s, 2H, CH_2CN), 3.76 (s, 3H, OMe); ^{13}C NMR ($CDCl_3$) δ: 158.0 (C*p*), 137.2 (C-7a), 132.3 (C*i*), 129.1 (C*o*), 127.3 (C-3a), 124.2 (C-2), 122.6 (C-6), 119.7 (C-5), 119.3 (C-4), 115.9 (CN), 114.0 (C*m*), 113.4 (C-3), 109.1 (C-7), 55.2 (OMe), 30.0 (NMe), 29.3 (CH_2Ph), 14.0 ($\underline{C}H_2CN$); IR ($CHCl_3$, cm^{-1}) ν_{max} = 2255, 1827; GC-MS (EI, 70 eV): *m*/*z* (%) = 290 (M^+, 100), 250 (9), 182 (43). HRMS: *m*/*z* calcd for $C_{19}H_{18}N_2O$ (M + Na) 313.1317, found 313.1320. For **11b**: R_f = 0.22 (hexane/CH_2Cl_2/EtOAc 50:48:2); ^{1}H NMR ($CDCl_3$) δ: 8.12 (br s, 1H, NH), 7.43 (dm, J = 7.9 Hz, 1H, H-4), 7.37 (dm, J = 8.1 Hz, 1H, H-7), 7.22 (ddd, J = 8.2, 7.0, 1.2 Hz, 1H, H-6), 7.09 (dm, J = 8.8 Hz, 2H, H*o*), 7.09 (overlapped, 1H, H-5); 6.80 (dm, J = 8.8 Hz, 2H, H*m*), 4.12 (q, J = 7.3 Hz, 1H, CHCN), 4.05 (AB, J = 16.4 Hz, 2H, CH_2Ph), 3.77 (s, 3H, OMe), 1.60 (d, J = 7.3 Hz, 3H, CH$\underline{Me}$); ^{13}C NMR ($CDCl_3$) δ: 158.0 (C*p*), 135.6 (C-7a), 132.1 (C*i*), 129.1 (C*o*), 128.8 (C-2), 128.3 (C-3a), 122.8 (C-6), 120.2 (CN), 120.1 (C-5), 119.3 (C-4), 113.9 (C*m*), 112.3 (C-3), 111.0 (C-7), 55.2 (OMe), 28.9 (CH_2Ph), 23.5 ($\underline{C}$HCN), 19.9 (CH$\underline{Me}$); IR ($CHCl_3$, cm^{-1}) ν_{max} = 3450, 2245, 1727; GC-MS (EI, 70 eV): *m*/*z* (%) = 290 (M^+, 100), 236 (68). HRMS: *m*/*z* calcd for $C_{19}H_{18}N_2O$ (M + Na) 313.1317, found 313.1319. For **11c**: R_f = 0.43 (hexane/CH_2Cl_2/EtOAc 50:48:2); ^{1}H NMR ($CDCl_3$) δ: 7.48 (dm, J = 7.9 Hz, 1H, H-4), 7.32 (dm, J = 8.1 Hz, 1H, H-7), 7.26 (ddd, J = 8.2, 7.0, 1.2 Hz, 1H, H-6), 7.09 (overlapped, 1H, H-5);7.07 (dm, J = 8.8 Hz, 2H, H*o*), 6.78 (dm, J = 8.8 Hz, 2H, H*m*), 4.28 (q, J = 7.3 Hz, 1H, CHCN), 4.11 (AB, J = 16.9 Hz, 2H, CH_2Ph), 3.89 (s, 3H, NMe), 3.76 (s, 3H, OMe), 1.54 (d, J = 7.3 Hz, 3H, CH$\underline{Me}$); ^{13}C NMR ($CDCl_3$) δ: 157.9 (C*p*), 137.4 (C-7a), 132.7 (C*i*), 130.0 (C-2), 129.0 (C*o*), 127.3 (C-3a), 122.5 (C-6), 120.0 (CN), 119.8 (C-5), 119.3 (C-4), 113.9 (C*m*), 112.3 (C-3), 109.1 (C-7), 55.2 (OMe), 30.7 (NMe), 29.1 (CH_2Ph), 22.1

(CHCN), 19.2 (CHMe); IR ($CHCl_3$, cm^{-1}) ν_{max} = 2245, 1846; GC-MS (EI, 70 eV): *m*/*z* (%) = 305 (M^+, 100), 251 (62), 197 (23). HRMS: *m*/*z* calcd for $C_{20}H_{20}N_2O$ (M + Na) 327.1473, found 327.1475.

*4.2.12. N-(2-(3-(4-Methoxybenzyl)-1H-indol-2-yl)ethyl)acetamide (**1c**).* A solution of **10** (150 mg, 0.5 mmol) was hydrogenated in a Parr bomb over W-2 Raney-Ni catalyst (substrate 30 mg/mL, catalyst 200% wt) in dry Ac_2O at room temperature under 45 psi H_2 for 6 h. The mixture was filtered through Celite and concentrated in vacuo to dryness. The residue was dissolved in CH_2Cl_2 (30 mL) and washed with water and brine. The organic layer was dried over Na_2SO_4, filtered, and concentrated in vacuo. The oil residue was purified by flash chromatography (hexane/EtOAc 1:4) to give **1c** (114 mg, 0.35 mmol, 65%) as unstable yellow oil. R_f = 0.28 (hexane/EtOAc 1:4); ^{1}H NMR ($CDCl_3$) δ: 8.52 (br s, 1H, NH), 7.43 (dm, *J* = 7.8 Hz, 1H, H-4), 7.33 (dm, *J* = 8.1 Hz, 1H, H-7), 7.14 (partial overlapped, 1H, H-5), 7.11 (dm, *J* = 8.8 Hz, 2H, H*o*), 7.05 (ddd, *J* = 8.2, 7.0, 1.2 Hz, 1H, H-6), 6.77 (dm, *J* = 8.8 Hz, 2H, H*m*), 5.40 (br t, *J* = 6.6 Hz, 1H, NHCO), 4.03 (s, 2H, CH_2Ph), 3.75 (s, 3H, OMe), 3.48 (q, *J* = 6.6 Hz, 2H, CH_2N), 2.95 (t, *J* = 6.6 Hz, 2H, CH_2C), 1.77 (s, 3H, COMe); ^{13}C NMR ($CDCl_3$) δ: 170.6 (C=O), 157.8 (C*p*), 135.6 (C-7a), 133.7 (C*i*), 132.5 (C-2), 129.0 (C*o*), 128.7 (C-3a), 121.5 (C-4), 119.4 (C-5), 118.6 (C-6), 113.8 (C*m*), 111.8 (C-3), 110.7 (C-7), 55.2 (OMe), 38.9 (CH_2N), 28.9 (CH_2Ph), 26.5(CH_2C), 23.1 (COMe); IR ($CHCl_3$, cm^{-1}) ν_{max} = 3453, 3310, 1670; GC-MS (EI, 70 eV): *m*/*z* (%) = 322 (M^+,100), (EI, 70 eV): *m*/*z* (%) = 264 (94), 249 (55). HRMS: *m*/*z* calcd for $C_{20}H_{22}N_2O_2$ (M + Na) 345.1579, found 345.1570.

*4.2.13. N-(2-(2-(4-Methoxybenzyl)-3-oxoindolin-2-yl)ethyl)acetamide (**12**).* Obtained by air oxidation of **1c** (100 mg, 0.31 mmol) upon standing (two months). Flash chromatography (CH_2Cl_2/AcOEt/MeOH 70:29:1) afforded **12** (103 mg, 0.30 mmol, 98%) as clear oil. R_f = 0.17 (hexane/EtOAc 1:4); ^{1}H NMR ($CDCl_3$) δ: 7.53 (br d, *J* = 8.1 Hz, H-4), 7.40 (ddd, *J* = 8.2, 7.0, 1.2 Hz, H-6), 7.06 (dm, *J* = 8.8 Hz, 2H, H*o*), 6.81 (partial overlapped, 1H, H-7), 6.77 (dm, *J* = 8.8 Hz, 2H, H*m*), 6.76 (partial overlapped, 1H, H-5), 5.49 (br t, *J* = 5.6 Hz, 1H, NHCO), 4.81 (br s, 1H, NH), 3.76 (s, 3H, OMe), 3.24 and 3.02 (2m, 2H, CH_2N), 2.82 (AB, *J* = 14.1 Hz, 2H, CH_2Ph), 2.09 and 1.87 (2m, 2H, CH_2C,), 1.81 (s, 3H, COMe); ^{13}C

NMR ($CDCl_3$) δ: 204.4 (C=O), 169.9 (NHC=O), 160.2 (C-7a), 158.7 (C*p*), 137.5 (C-6), 131.2 (C*o*), 127.3 (C*i*), 124.4 (C-4), 120.7 (C-3a), 118.9 (C-5), 113.7 (C*m*), 112.4 (C-7), 69.0 (C-2), 55.2 (OMe), 42.5 (CH_2Ph), 35.5 ($\underline{C}H_2C$), 34.9 (CH_2N), 23.2 (CO$\underline{Me}$); IR ($CHCl_3$, cm^{-1}) ν_{max} = 3441, 3340, 1675, 1618, GC-MS (EI, 70 eV): *m*/*z* (%) = 338 (M^+, 4), 217 (19), 158 (100); HRMS: *m*/*z* calcd for $C_{20}H_{22}N_2O_3$ (M + Na) 361.1528, found 361.1530.

4.2 Crystallographic studies

The X-ray data of **3a** were measured on a Bruker Smart 6000 CCD diffractometer using Mo Ka radiation (λ = 0.71073 Å). The X-ray data of **3b**, **8** and **10a** were collected on a Bruker-Nonius CAD4 diffractometer using Cu Kα radiation (λ = 1.54184 Å). The data were collected in the ω-2θ scan mode. Unit cell refinements were done using CAD4 Express v 2.0 software and structures were solved by direct methods using SHELXS-97 program included in the WinGX v 1.64.05 crystallographic software package. For the structural refinement, the non-hydrogen atoms were treated anisotropically, and the hydrogen atoms, included in the structure factor calculation, were refined isotropically. CCDC 1469876-1469879 contains the supplementary crystallographic data for this paper. These data can be obtained free of charge via http://www.ccdc.cam.ac.uk/conts/retrieving.html.

Acknowledgements

The present work is partially supported by CONACYT grant 179187 and Programa de Fortalecimiento Académico del Posgrado de Alta Calidad.

Appendix. Supplementary data

The following are the supplementary data related to this article: ^1H and ^{13}C NMR spectra of new compounds, X-ray crystallographic data, pharmacophore models building, and computational data.

REFERENCES

[1] G. Tosini, S. Owino, J.L. Guillaume, R. Jockers, Understanding melatonin receptor pharmacology: Latest insights from mouse models, and their relevance to human disease, Bioessays 36 (2014) 778-787. DOI: 10.1002/bies.201400017

[2] D. Acuña-Castroviejo, G. Escames, C. Venegas, M.E Díaz-Casado, E. Lima-Cabello, L.C. López, S. Rosales-Corral., D.-X. Tan, R.J. Reiter, Extrapineal melatonin: sources, regulation, and potential functions, Cell Mol. Life Sci. 71 (2014) 2997-3025. DOI: 10.1007/s00018-014-1579-2

[3] P. Delagrange, B. Guardiola-Lemaitre, Melatonin, its receptors, and relationships with biological rhythm disorders, Clin. Neuropharmacol. 20 (1997) 482-510. DOI: 10.1097/00002826-199712000-00002

[4] M.L. Dubocovich, P. Delagrange, D.N. Krause, D. Sugden, D.P. Cardinali, J. Olcese, International Union of Basic and Clinical Pharmacology. LXXV. Nomenclature, classification, and pharmacology of G protein-coupled melatonin receptors, Pharmacol. Rev. 62 (2010) 343-380. DOI: 10.1097/00002826-199712000-00002

[5] G. O'Neal-Moffitt, J. Pilli, S.S. Kumar, J. Olcese, Genetic deletion of MT1/MT2 melatonin receptors enhances murine cognitive and motor performance, Neuroscience 277 (2014) 506-521. DOI: 10.1016/j.neuroscience.2014.07.018

[6] C. Karaaslan, S. Suzen, Antioxidant properties of melatonin and its potential action in diseases, Curr. Top. Med. Chem. 15 (2015) 894-903. DOI: 10.2174/1568026615666150220129 46

[7] J.J. García, L. López-Pingarrón, P. Almeida-Souza, A. Tres, P. Escudero, F.A. García-Gil, D.X. Tan, R.J. Reiter, J.M. Ramírez, M. Bernal-Pérez, Protective effects of melatonin in reducing oxidative stress and in preserving the fluidity of biological membranes: a review, J. Pineal Res. 56 (2014) 225-237. DOI: 10.1111/jpi.12128

[8] A. Galano, D.X. Tan, R.J. Reiter, On the free radical scavenging activities of melatonin's metabolites, AFMK and AMK, J. Pineal Res. 54 (2013) 245-257. DOI: 10.1111/jpi.12010

[9] R.J. Reiter, J.M. Guerrero, J.J. Garcia, D. Acuna-Castroviejo, Reactive oxygen intermediates, molecular damage, and aging: relation to melatonin, Ann. N. Y. Acad. Sci. 854 (1998) 410-24. DOI: 10.1111/j.1749-6632.1998.tb09920.x

[10] P.M. Abuja, P. Liebmann, M. Hayn, K. Schauenstein, H. Erstebauer, Antioxidant role of melatonin in lipid peroxidation of human LDL, FEBS Letters 413 (1997) 289-293. DOI:10.1016/S0014-5793(97)00918-6

[11] B. Le Bars, P. Thivolle, P.A. Vitte, C. Bojkowski, G. Chazot, J. Arendt. R.S.J. Frackowiak, B. Claustrat, PET and plasma pharmacokinetic studies after bolus intravenous administration of [^{11}C] melatonin in humans, Int. J. Rad. Appl. Instrum. B 18 (1991) 357-62. DOI: 10.1016/0883-2897(91)90132-5

[12] P.J. Garratt, A. Tsotinis, Synthesis of compounds as melatonin agonists and antagonists, Mini-Rev. Med. Chem. 10 (2007) 1075-1088. DOI: 10.2174/138955707782110132

[13] D.P. Zlotos, Recent advances in melatonin receptor ligands, Arch. Pharm. 338 (2005) 229-247. DOI: 10.1002/ardp.200400996

[14] A. Carocci, A. Catalano, A. Angelo-Lovece, G. Lentini, A. Duranti, V. Lucini, M. Marilou Pannacci, F. Scaglione, C. Franchini, Design, synthesis, and pharmacological effects of structurally simple ligands for MT1 and MT2 melatonin receptors, Bioor. Med. Chem. 18 (2010) 6496-6511. DOI: 10.1016/j.bmc.2010.06.100

[15] P.J. Garratt, S. Travard, S. Vonhoff, A. Tsotinis, D.J. Sugden, Mapping the melatonin receptor. 4. Comparison of the binding affinities of a series of substituted phenylalkyl amides, J. Med. Chem. 39 (1996) 1797-1805. DOI: 10.1021/jm9508189

[16] M. Langlois, B. Brémont, S. Shen, A. Poncet, J. Andrieux, S. Sicsic, I. Serraz, M. Mathé-Allainmat, P. Renard, P. Delagrange, Design and synthesis of new naphthalenic derivatives as ligands for 2-[^{125}I]iodomelatonin binding sites, J. Med. Chem. 38 (1995) 2050-2060. DOI: 10.1021/jm00012a004

[17] M. Mor, P.V. Plazzi, G. Spadoni, G. Tarzia, Melatonin, Curr. Med. Chem. 6 (1999) 501-518.

[18] G. Tarzia, G. Diamantini, G. Spadoni, Indole melatonin agonists and antagonists derived by shifting the melatonin side chain from the C-3 to the N-1 or to the C-2 indole, Biol. Signals Recept. 8 (1999) 24-31. DOI:10.1159/000014565

[19] G. Wolber, T. Langer, LigandScout: 3-D pharmacophores derived from protein-bound ligands and their use as virtual screening filters, J. Chem. Inf. Model 45 (2005) 160-169. DOI: 10.1021/ci049885e

[20] D. Pala, T. Beuming. W. Sherman, A. Lodola, S. Rivara, M. Mor, Structure-based virtual screening of MT2 melatonin receptor: Influence of template choice and structural refinement, J. Chem. Inf. Model 53 (2013) 821-835. DOI: 10.1021/ci4000147

[21] J.M. Jansen, S. Copinga, G. Gruppen, E.J. Molinari, M.L. Dubocovich, C.J. Grol, The high affinity melatonin binding site probed with conformationally restricted ligands-I. Pharmacophore and minireceptor models, Bioorg. Med. Chem. 4 (1996) 1321-1332. DOI: 10.1016/0968-0896(96)00113-7

[22] G. Spadoni, C. Balsamini, G. Diamantini, A. Tontini, G. Tarzia, M. Mor, S. Rivara, P.V. Plazzi, R. Nonno, V. Lucini, M. Pannacci, F. Fraschini, B.M. Stankov, 2-*N*-Acylaminoalkylindoles: design and quantitative structure-activity relationship studies leading to MT2-selective melatonin antagonists, J. Med. Chem. 44 (2001) 2900-912. DOI: 10.1021/jm001125h

[23] M. Mor, G. Spadoni, B. Di Giacomo, G. Diamantini, A. Bedini, G. Tarzia, P.V. Plazzi, S. Rivara, R. Nonno, V. Lucini, M. Pannacci, F. Fraschini, B.M. Stankov, Synthesis, pharmacological characterization and QSAR studies on 2-substituted indole melatonin receptor ligands, Bioorg. Med. Chem. 9 (2001) 1045-1057. DOI: 10.1016/S0968-0896(00)00322-9

[24] V. Lucini, M. Pannacci, F. Scaglione, F. Fraschini, S. Rivara, M. Mor, F. Bordi, P.V. Plazzi, G. Spadoni, A. Bedini, G. Piersanti, G. Diamantini, G. Tarzia, Tricyclic alkylamides as melatonin receptor ligands with antagonist or inverse agonist activity, J. Med. Chem. 47 (2004) 4202−4212. DOI: 10.1021/jm040768k

[25] A. Bedini, S. Lucarini, G. Spadoni, G. Tarzia, F. Scaglione, S. Dugnani, M. Pannacci, V. Lucini, C. Carmi, D. Pala, S. Rivara, M. Mor, Toward the definition of stereochemical requirements for MT2-selective antagonists and partial agonists by studying 4-phenyl-2-propionamidotetralin derivatives, J. Med. Chem. 54 (2011): 8362-8372. DOI: 10.1021/jm200790v

[26] Gaussian 03, Revision C.02, M.J. Frisch, G.W. Trucks, H.B. Schlegel, G.E. Scuseria, M.A. Robb, J.R. Cheeseman, J.A. Montgomery, Jr., T. Vreven, K.N. Kudin, J.C. Burant, J.M. Millam, S.S. Iyengar, J. Tomasi, V. Barone, B. Mennucci, M. Cossi, G. Scalmani, N. Rega, G.A. Petersson, H. Nakatsuji, M. Hada, M. Ehara, K. Toyota, R. Fukuda, J. Hasegawa, M. Ishida, T. Nakajima, Y. Honda, O. Kitao, H. Nakai, M. Klene, X. Li, J.E. Knox, H.P. Hratchian, J.B. Cross, V. Bakken, C. Adamo, J. Jaramillo, R. Gomperts, R.E. Stratmann, O. Yazyev, A.J. Austin, R. Cammi, C. Pomelli, J.W. Ochterski, P.Y. Ayala, K. Morokuma, G.A. Voth, P. Salvador, J.J. Dannenberg, V.G. Zakrzewski, S. Dapprich, A.D. Daniels, M.C. Strain, O. Farkas, D. K. Malick, A.D. Rabuck, K. Raghavachari, J.B. Foresman, J.V. Ortiz, Q. Cui, A.G. Baboul, S. Clifford, J. Cioslowski, B.B. Stefanov, G. Liu, A. Liashenko, P. Piskorz, I. Komaromi, R.L. Martin, D.J. Fox, T. Keith, M.A. Al-Laham, C.Y. Peng, A. Nanayakkara, M. Challacombe, P.M.W. Gill, B. Johnson, W. Chen, M.W. Wong, C. Gonzalez, and J.A. Pople, Gaussian, Inc., Wallingford CT, 2004.

[27] Gaussian 09, Revision E.01, M.J. Frisch, G.W. Trucks, H.B. Schlegel, G.E. Scuseria, M.A. Robb, J.R. Cheeseman, G. Scalmani, V. Barone, B. Mennucci, G.A. Petersson, H. Nakatsuji, M. Caricato, X. Li, H.P. Hratchian, A.F. Izmaylov, J. Bloino, G. Zheng, J.L. Sonnenberg, M. Hada, M. Ehara, K. Toyota, R. Fukuda, J. Hasegawa, M. Ishida, T. Nakajima, Y. Honda, O. Kitao, H. Nakai, T. Vreven, J.A. Montgomery, Jr., J.E. Peralta, F. Ogliaro, M. Bearpark, J.J. Heyd, E. Brothers, K.N. Kudin, V.N. Staroverov, R. Kobayashi, J. Normand, K. Raghavachari, A. Rendell, J.C. Burant, S.S. Iyengar, J. Tomasi, M. Cossi, N. Rega, J.M. Millam, M. Klene, J.E. Knox, J.B. Cross, V. Bakken, C. Adamo, J. Jaramillo, R. Gomperts, R.E. Stratmann, O. Yazyev, A.J. Austin, R. Cammi, C. Pomelli, J.W. Ochterski, R.L. Martin, K. Morokuma, V. G. Zakrzewski, G.A. Voth, P. Salvador, J.J. Dannenberg, S. Dapprich, A.D. Daniels, Ö. Farkas, J.B. Foresman, J.V. Ortiz, J. Cioslowski, and D.J. Fox, Gaussian, Inc., Wallingford CT, 2009.

[28] S. Horowitz, R.C Trievel, Carbon-oxygen hydrogen bonding in biological structure and function, J. Biol. Chem. 287 (2012) 41576-41582. DOI: 10.1074/jbc.R112.418574

[29] D. Peters, J. Peters, Quantum theory of the structure and bonding in proteins: Part 6 Factors governing the formation of hydrogen bonds in proteins and peptides, J. Mol. Struct. 68 (1980) 255-270. DOI: 10.1016/0022-2860(80)80277-8

[30] G.R. Desiraju, The C-H···O hydrogen bond: structural implications and supramolecular design, Acc. Chem. Res. 29 (1996) 441-449. DOI: 10.1021/ar950135n

[31] P.I. Nagy, Competing intramolecular vs intermolecular hydrogen bonds in solution, Int. J. Mol. Sci. 15 (2014) 19562-19633. DOI: 10.3390/ijms151119562

[32] S.H. Gellman, G.P. Dado, G.B. Liang, B.R. Adams, Conformation-directing effects of a single intramolecular amide-amide hydrogen bond: variable-temperature NMR and IR studies on a homologous diamide series, J. Am. Chem. Soc. 113 (1991) 1164-1173. DOI: 10.1021/ja00004a016

[33] S. Rivara, S. Lorenzi, M. Mor, P.V. Plazzi, G. Spadoni, A. Bedini, G. Tarzia, Analysis of structure-activity relationships for MT_2 selective antagonists by melatonin MT_1 and MT_2 receptor models, J. Med. Chem. 48 (2005) 4049-4060. DOI: 10.1021/jm048956y

[34] G. Tarzia, G. Diamantini, B. Di Giacomo, G. Spadoni, 1-(2-Alkanamidoethyl)-6-methoxyindole derivatives: A new class of potent indole melatonin analogues, J. Med. Chem. 40 (1997) 2003-2010. DOI: 10.1021/jm960653j

[35] G. Spadoni, C. Balsamini, A. Bedini, G. Diamantini, B. Di Giacomo, A. Tontini, G. Tarzia, 2-[N-Acylamino(C1-C3)alkyl]indoles as MT1 melatonin receptor partial agonists, antagonists, and putative inverse agonists, J. Med. Chem. 41 (1998) 3624-3634. DOI: 10.1021/jm970721h

[36] M Bandini, Electrophilicity: the “dark-side” of indole chemistry, Org. Biomol. Chem. 11 (2013) 5206-5212. DOI: 10.1039/c3ob40735g.

[37] Y. Miki, H. Hachiken, Y. Kashima, W. Sugimura, N. Yanase, *p*-Methoxybenzyl group as a protecting group of the nitrogen in indole derivatives: deprotection by DDQ of trifluoroacetic acid, Heterocycles 48 (1998) 1-4. DOI: 10.3987/COM-97-7990

[38] G. Spadoni, G. Diamantini, A. Bedini, G. Tarzia, F. Vacondio, C. Silva, M. Rivara, M. Mor, P.V. Plazzi, M. Zusso, D. Franceschini, P. Giusti, Synthesis, antioxidant activity and structure-activity relationships for a new series of 2-(N-acylaminoethyl)indoles with melatonin-like cytoprotective activity, J. Pineal Res. 40 (2006) 259-269. DOI: 10.1111/j.1600-079X.2005.00309.x

[39] S.M. Kerwin, ChemBioOffice Ultra 2010 Suite, J. Am. Chem. Soc. 132 (2010) 2466-2467. DOI: 10.1021/ja1005306

[40] T.A. Halgren, Merck molecular force field. I. Basis, form, scope, parameterization, and performance of MMFF94, J. Comput. Chem. 17 (1996) 490-519. DOI: 10.1002/(SICI)1096-987X(199604)17:5/6<490::AID-JCC1>3.0.CO;2-P

[41] W. Hehre, A guide to molecular mechanics and quantum chemical calculations, Wavefunction, Inc., (1993) http://www.wavefun.com/japan/products/books/AGuidetoMM_Cha1-2.pdf.

[42] Spartan '04; Wavefunction, Inc.: Irvine, CA, 2004.

[43] A.D. Becke, Density-functional thermochemistry. III. The role of exact exchange, J. Chem. Phys. 55 (1993) 117-129. DOI: 10.1007/978-3-662-10421-7_60

[44] C. Lee, W. Yang, R.G. Parr, Development of the Colle-Salvetti correlation-energy formula into a functional of the electron density, Phys. Rev. B. 37 (1998) 785-788. DOI: http://dx.doi.org/10.1103/PhysRevB.37.785

[45] Spartan'14 for Windows, Macintosh, and Linux; Wavefunction, Inc., http://downloads.wavefun.com/Spartan14Manual.pdf.

[46] S. Miertus, E. Scrocco, J. Tomasi, Electrostatic interaction of a solute with a continuum. A direct utilization of AB initio molecular potentials for the prevision of solvent effects, J. Chem. Phys. 55 (1981) 117-129. DOI: 10.1016/0301-0104(81)85090-2

[47] V. Barone, M. Cossi, J. Tomasi, A new definition of cavities for the computation of solvation free energies by the polarizable continuum model, J. Chem. Phys. 107 (1997) 3210-3221. DOI: 10.1063/1.474671

[48] M. Caricato, B. Mennucci, J. Tomasi, F. Ingrosso, R. Cammi, S. Corni, G. Scalmani, Formation and relaxation of excited states in solution: A new time dependent polarizable continuum model based on time dependent density functional theory, J. Chem. Phys. 124 (2006) 124520-124532. DOI: http://dx.doi.org/10.1063/1.2183309

[49] N.A. Kogan, M.I. Vlasova, Synthesis and properties of 1,2-dihydropyridazino[4,5-b]indole, Chem. Heterocycl. Compd. 10 (1974) 679-682. DOI: 10.1007/BF00480923, Translated from Khim. Geterotsikl. Soedin 12 (1973) 1654-1658.

Highligths

New 2-(*N*-acylaminoalkyl)indoles have been synthesized and characterized

Optimized geometry and theoretical calculations have been computed using DFT methods

Conformational dependence in the gas phase and in aqueous solution has been investigated

Pharmacophoric properties indicate their ability as antagonist melatoninergic ligands